Circulating MicroRNA-122 Is Associated With The Risk of New-Onset Metabolic Syndrome And Type-2-Diabetes

Running title: MicroRNA-122 and new-onset metabolic diseases

Authors: Peter Willeit[1,2,3], Philipp Skroblin[1], Alexander R. Moschen[4], Xiaoke Yin[1], Dorothee Kaudewitz[1], Anna Zampetaki[1], Temo Barwari[1], Meredith Whitehead[1], Cristina M. Ramírez[5], Leigh Goedeke[5], Noemi Rotllan[5], Enzo Bonora[6], Alun D. Hughes[7], Peter Santer[8], Carlos Fernández-Hernando[5], Herbert Tilg[4], Johann Willeit[2], Stefan Kiechl[2], Manuel Mayr[1]

Affiliations: [1]King's British Heart Foundation Centre, King's College London, United Kingdom; [2]Department of Neurology, Medical University of Innsbruck, Innsbruck, Austria; [3]Department of Public Health and Primary Care, University of Cambridge, United Kingdom; [4]Department of Internal Medicine I, Gastroenterology, Endocrinology & Metabolism, Medical University Innsbruck, Innsbruck, Austria; [5]Vascular Biology and Therapeutics Program, Yale University School of Medicine, New Haven, CT, USA; [6]Division of Endocrinology, Diabetes and Metabolic Diseases, University and Hospital Trust of Verona, Verona, Italy; [7]Institute of Cardiovascular Sciences, University College London, London, UK; and [8]Department of Laboratory Medicine, Bruneck Hospital, Bruneck, Italy.

Corresponding authors: Peter Willeit, Department of Neurology, Medical University of Innsbruck, Anichstraße 35, 6020 Innsbruck, Austria, peter.willeit@i-med.ac.at; or Manuel Mayr, King's British Heart Foundation Centre, King's College London, 125 Coldharbour Ln, London SE5 9NU, United Kingdom, manuel.mayr@kcl.ac.uk.

3892 words, **1** table, **5** figures, **1** Supplementary material

Diabetes Publish Ahead of Print, published online November 29, 2016

ABSTRACT

MicroRNA-122 (miR-122) is abundant in the liver and involved in lipid homeostasis, but its relevance to the long-term risk of developing metabolic disorders is unknown. We therefore measured circulating miR-122 in the prospective population-based Bruneck Study (*n*=810; survey year: 1995). Circulating miR-122 was associated with prevalent insulin resistance, obesity, metabolic syndrome, type-2 diabetes, and an adverse lipid profile. Among 92 plasma proteins and 135 lipid subspecies quantified with mass spectrometry, it correlated inversely with zinc-alpha-2-glycoprotein and positively with afamin, complement-factor H, VLDL-associated apolipoproteins, and lipid subspecies containing monounsaturated and saturated fatty acids. Proteomics analysis of livers from antagomiR-122-treated mice revealed novel regulators of hepatic lipid metabolism that are responsive to miR-122 inhibition. In the Anglo-Scandinavian Cardiac Outcomes Trial (ASCOT, *n*=155), 12-month atorvastatin reduced circulating miR-122. A similar response to atorvastatin was observed in mice and cultured murine hepatocytes. Over up to 15 years of follow-up in the Bruneck Study, multivariable adjusted risk ratios per 1-SD higher log miR-122 were 1.60 (95% confidence interval: 1.30-1.96; *P*<0.001) for metabolic syndrome and 1.37 (1.03-1.82; *P*=0.021) for type-2 diabetes. In conclusion, circulating miR-122 is strongly associated with the risk of developing metabolic syndrome and type-2 diabetes in the general population.

MicroRNAs (miRNAs) are small non-coding RNA molecules that regulate gene expression (1). The predominant miRNA in the liver, microRNA-122 (miR-122), has been proposed to play a central role in the regulation of lipid and glucose metabolism (2,3). Inhibition of miR-122 in mice (4,5) and non-human primates (6,7) induces fatty acid oxidation, reduces lipid synthesis, and thereby leads to lower levels of total cholesterol.

In humans, it has been suggested that miR-122 may have adverse metabolic effects and may be associated with metabolic diseases. However, as highlighted by our recent review (3), evidence from existing epidemiological studies is sparse and has important limitations. Published studies have focused on correlations with major lipids (8), whereas a breakdown into lipid subspecies would add resolution and help improve our understanding of the regulation of lipid homeostasis by miR-122. Importantly, previous studies had cross-sectional or case-control designs (3) and hence were unable to inform about long-term associations of circulating miR-122 with the development of new-onset disease outcomes over time.

To address this gap in the current literature, we conducted a series of analyses in the prospective Bruneck Study, the randomised controlled Anglo-Scandinavian Cardiac Outcomes Trial (ASCOT), and experiments in mice and cell culture, combining lipidomics, proteomics, and miR-122 data. Our aims were four-fold. First, to assess cross-sectional correlates of circulating miR-122, including lipidomics and proteomics profiles. Second, to provide mechanistic insight into the putative regulatory function of miR-122 in lipid metabolism with animal studies of antagomiR-122 interventions and statin treatment. Third, to study the effect of statin allocation on serum miR-122 in participants of ASCOT. Fourth, to quantify the – to date unknown – associations of circulating miR-122 with the long-term risk of developing metabolic syndrome and type-2 diabetes (T2DM).

RESEARCH DESIGN AND METHODS

The Bruneck Study

The Bruneck Study is a prospective, population-based study (9-13). In 1990, 1,000 individuals aged 40 to 79 years were recruited as a random sample of Bruneck inhabitants and were re-examined every 5 years since, with participation rates exceeding 90% at all surveys. The present study used the 1995 survey as baseline. Full medical records were available on clinical endpoints occurring between 1995 and 2010 (1995-2005 for metabolic syndrome) for all individuals, including those who did not participate in later evaluations or died during follow-up (100% follow-up for clinical endpoints). Metabolic syndrome was diagnosed if three out of the five following characteristics were present: (i) waist circumference in men ≥102 cm and women ≥88 cm; (ii) fasting triglycerides ≥150 mg/dl or on drug treatment for elevated triglycerides (fibrates and nicotinic acids); (iii) HDL cholesterol in men <40 and women <50 mg/dl or on drug treatment for reduced HDL cholesterol (fibrates and nicotinic acids); (iv) blood pressure ≥130/≥85 mmHg or antihypertensive drug treatment in a patient with a history of hypertension; and (v) fasting glucose ≥100 mg/dl or on drug treatment for elevated glucose. T2DM was diagnosed according to 1997 American Diabetes Association criteria or if the participant had a clinical diagnosis of T2DM and received anti-diabetic treatment. CVD was defined as myocardial infarction, stroke, or vascular death. Fatal and nonfatal myocardial infarction were deemed confirmed when World Health Organization criteria for definite disease status were met. Ischaemic stroke and transient ischaemic attacks were classified according to the criteria of the National Survey of Stroke. Self-report of disease was always confirmed by reviewing the participant's medical records available from their general practitioners and the Bruneck Hospital.

Risk factors were ascertained by validated standard procedures as previously described (9-13). Socioeconomic status was defined on a three-category scale (low, medium or high) on the basis of information on occupational status and educational level of the person with the highest income in the household. High socioeconomic status was assumed if the participant had ≥12 years of education or an occupation with an average monthly income ≥$2,000 (baseline salary before tax). Low socioeconomic status was defined by ≤8 years of education or an average monthly income ≤$1,000. Physical activity was assessed using the validated Baecke Score (14). Waist and hip circumferences were assessed with a plastic tape measure at the levels of the umbilicus and the greater trochanters respectively. Blood samples were taken after an overnight fast. Lipidomics profiling in plasma samples of the Bruneck cohort was performed with mass spectrometry, which allowed quantification of 135 distinct lipid species (9). HbA1c was quantified using high performance liquid chromatography (DCCT-aligned assay). The degree of insulin resistance by homeostasis model assessment (HOMA-IR) was estimated using the formula fasting plasma glucose in mmol/l × fasting serum insulin in mU/l divided by 22.5, with higher HOMA-IR values indicating higher insulin resistance (15). MiR-122 was measured in serum taken at the 1995 examination (n=810) as well as in serum and plasma taken at the 2000 examination (n=695).

The Anglo-Scandinavian Cardiac Outcomes Trial (ASCOT)

ASCOT is a double-blind randomised 2x2 factorial study of blood-pressure-lowering and lipid-lowering treatment (16-18). A total of 14,412 patients (aged 40-79 years) were randomized between 1998 and 2000 using a computer-generated optimum allocation mechanism blinded for any person involved in the undertaking of the study. Patients randomized to the lipid-lowering arm had low to moderate cholesterol levels (serum total cholesterol≤6.5 mmol/l) and were allocated atorvastatin (10mg/day) or placebo. Serum miR-

122 levels were measured at baseline and 1 year after randomisation (median 13 [range 12 to 16] months) in participants of the hypertension-associated cardiovascular disease sub-study (HACVD-ASCOT) who were of European ancestry and did not have T2DM at study entry.

AntagomiR Treatment in Mice

Mice were injected intraperitoneally with antagomiR-122 and control antagomiRs (65 mg/kg; n = 5 per group) on three consecutive days as previously described (19). AntagomiRs were purchased from Fidelity Systems with the following sequences: antagomiR-122 - C*A*AACACCAUUGUCACACU*C*C*A*Chol*-T; controls - A*A*GGCAAGCUGACCUGAA*G*U*U*Chol-T. Mice were sacrificed at day 7. Liver and serum samples were harvested for analysis. Total and HDL-cholesterol were enzymatically measured using the T-Cholesterol and HDL-C Assay Kits (Wako Diagnostics) with blood samples were collected by retro-orbital venous plexus puncture after a 12h overnight fast. We measured hepatic miRNA-122 expression using Northern blot, and miR-122 and other miRNAs in liver and serum using quantitative reverse transcription real time polymerase-chain reaction (qRT-PCR). Selected genes were also quantified by qRT-PCR (for details, see Supplementary material online).

Statin Treatment in Mice and Primary Murine Hepatocytes

Six-week old, female C57Bl/6 mice were injected once a day with 20mg/kg atorvastatin intraperitoneally (Sigma Aldrich, Taufkirchen, Germany) for 5 days, and were sacrificed on day 5. Serum was collected by cardiac puncture. The liver was perfused with ice-cold phosphate-buffered saline and tissue specimens from the left lower lobe were either snap frozen or placed in RNAlater (Qiagen, Hilden, Germany) until further processing. Details are provided in the Supplementary material online.

Proteomics Analyses

Targeted proteomics profiling in plasma samples of the Bruneck Study (year 2000 evaluation) was performed using multiple reaction monitoring (PlasmaDive kits, Biognosys AG), which allowed quantification of 92 proteins (for details, see Supplementary material online). During continuous operation over 2 weeks, the inter-day relative standard deviation was <20% and <5% without and with adjustment for the peak area of the authentic standard peptides, respectively.

Proteomic analysis of livers from antagomiR-treated mice was performed after an in-solution digest by liquid chromatography tandem mass spectrometry (LC-MS/MS). Differential protein expression was assessed by two methods (for details, see Supplementary material online): by spectral counting using a high mass accuracy instrument (Q-Exactive HF, ThermoFisher) and by labelling with TMT Mass Tags (ThermoFisher) using the triple-stage mass spectrometry (MS3) capability on an Orbitrap Fusion Tribrid MS (ThermoFisher). MS3 can overcome the inherent interference of more commonly used two-stage (MS2) workflows when isobaric labeling strategies are used with complex samples (20).

miR-122 Measurement using Quantitative Real-time PCR (qRT-PCR)

We measured miRNA-122 in samples of the Bruneck Study, ASCOT and statin experiments using qRT-PCR, as previously described (11,21). Briefly, total RNA was extracted using the miRNeasy kit (Qiagen, Hilden, Germany). For plasma, serum or cell culture supernatants, a fixed volume of 3µl of the 25µl RNA eluate was used as input for reverse transcription (RT) reactions. For RNA from cells or tissue, 100ng input material was used for RT. MiRNAs were reversely transcribed using Megaplex Primer Pools (Human Pool A version 2.1 or Rodent Pool A, Life Technologies, Darmstadt, Germany) and products were further amplified using Megaplex PreAmp Primers (Primers A v2.1). Both RT and PreAmp products

were stored at -20°C. Taqman miRNA assays were used to assess the expression of individual miRNAs. Diluted pre-amplification product (0.5µl) or RT product (corresponding to 0.45ng input) were combined with 0.25µl Taqman microRNA assay (20×) (Life Technologies) and 2.5µl Taqman Universal PCR Master Mix No AmpErase UNG (2×) to a final volume of 5µl. qRT-PCR was performed on an Applied Biosystems 7900HT thermocycler at 95°C for 10min, followed by 40 cycles of 95°C for 15s and 60°C for 1min. All samples were run in duplicate. Laboratory technicians were blinded to the participants' disease status. Relative quantification was performed using the software SDS2.2 (Life Technologies). U6 and exogenous *C. elegans* spike-in control (Cel-miR-39) were used for normalization purposes in cell and tissue experiments. For conditioned media, normalization was achieved by cultivating the same cell number in the same volume of medium with the spike-in control being used to adjust for any experimental variability in the isolation procedure.

Statistical Analysis

The statistical analysis was conducted according to a pre-specified analysis plan. MiR-122 values were log-transformed for analysis. Cross-sectional associations of miR-122 levels with other participant characteristics were quantified using Spearman correlation coefficients and linear regression models adjusted for age and sex. In the survival analysis, the principal outcomes were metabolic syndrome and T2DM, and a secondary outcome was CVD. We used Cox proportional hazard regression with updated covariates for CVD and T2DM and pooled logistic regression (22) for metabolic syndrome. Both techniques make full use of the repeat measurements of miR-122 available at the 1995 and 2000 examination. Hazard ratios and odds ratios were assumed to represent the same measure of relative risk and are collectively described as risk ratios (RR). Participants with prevalent disease were excluded

from the respective analyses. Models were adjusted for age and sex, plus socio-economic status (low, medium, high), smoking (yes, no), physical activity and alcohol consumption ("multivariable model"). A sensitivity analysis further adjusted for the potential mediators/confounders body mass index and waist-hip ratio. The proportional hazards assumption for CVD and T2DM was tested using Schoenfeld residuals and was met. We investigated effect modification with formal tests for interaction across groups defined by age, sex, statin intake, and obesity. Principal analyses used significance levels of two-sided $P<0.05$. Exploratory analyses used Bonferroni-corrected P values to limit the risk of false-positive results (i.e. 0.00037 for analyses of lipid subspecies; 0.00054 for proteins; 0.0042 for interaction tests). Analyses were performed using Stata software, version 12.1.

Study Approval

The Bruneck Study protocol was approved by the local ethic committee of Bolzano ('Comitato etico del comprensorio sanitario di Bolzano'; approval number 28–2010). The ASCOT protocol was approved by central and regional ethics review boards in the UK and by national ethics and statutory bodies in Ireland and the Nordic countries. Animal experiments were approved by the Austrian authorities (licensed to A. R. Moschen No BMWF-66.011/0040-II/10b/2009) and UK authorities (licensed to Q. Xu No. PPL70/7266). The participants' written informed consent was obtained prior to their inclusion in the Bruneck and ASCOT studies.

RESULTS

miR-122 and Major Clinical Characteristics in Participants of the Bruneck Study

We successfully quantified circulating miR-122 levels in 810 out of 826 participants of the Bruneck Study. MiR-122 levels in serum and plasma were strongly correlated (r = +0.86; 95% confidence interval: 0.84-0.88). The within-person correlation of repeat serum miR-122 measurements taken five years apart was +0.24 (0.17-0.31; Supplementary Fig. 1), which is comparable to the range previously reported for other plasma miRNAs (23). Table 1 shows baseline clinical characteristics of the Bruneck participants and their correlations with miR-122. The mean age of participants was 63 years (SD, 11) and 50% were female. Circulating miR-122 was associated with higher levels of liver enzymes, adiposity, inflammation, insulin resistance, and an adverse lipid profile (higher triglycerides and lower HDL-C) (Table 1). Participants with a diagnosis of metabolic syndrome compared to those without had 160% higher circulating miR-122 levels (P<0.001); participants with a diagnosis of T2DM compared to those without had 214% higher circulating miR-122 levels (P<0.001). No difference in circulating miR-122 levels was observed in participants with a history of CVD compared to participants without a history of CVD (P=0.969).

miR-122 and Lipidomic and Proteomic Profiles in Participants of the Bruneck Study

To provide novel insight into the complex correlation patterns of miR-122 beyond those with major clinical characteristics, we quantified cross-sectional correlations of miR-122 with lipidomic and proteomic profiles. Of the 135 distinct lipid subspecies available in the Bruneck Study (9), miR-122 showed a specific correlation with lipid subspecies comprised of monounsaturated and saturated fatty acids within the lipid classes triacylglycerols and cholesterol esters (Fig. 1*A*).

The proteomics assessment, over 4 orders of magnitude in abundance by mass spectrometry, covered 92 plasma proteins, including apolipoproteins, complement and coagulation factors (Fig. 1*B*; for full results, see Supplementary Fig. 2). Circulating miR-122 was most strongly associated with afamin (r=+0.42; P=$4x10^{-30}$), complement factor H (r=+0.21; P=$3x10^{-8}$), and zinc-alpha-2-glycoprotein (r=-0.28; P=10^{-13}). Focused analyses of apolipoproteins revealed significant positive correlations with APOB, APOC2, APOC3, APOE, and APOL1, and significant inverse correlations with APOA4 and APOD.

Treatment with AntagomiR-122 in Mice and Effect on the Hepatic Proteome

To scrutinise the role of miR-122 in the regulation of hepatic lipid metabolism, we inhibited miR-122 in mice using antagomiRs and studied consequences thereof at the miRNA, lipid, gene expression, and protein level. AntagomiR-122 led to an almost complete inhibition of miR-122 expression (Fig. 2*A*), with a secondary effect on hepatic miR-33 expression, but no effects on the expression of other miRNAs relevant to the hepatic liver metabolism, including miR-27b and miR-148a (Fig. 2*B*). The marked inhibition of hepatic miR-122 expression by antagomiR-122 treatment was reflected in a >10-fold reduction in the mean serum levels of circulating miR-122 (P=0.032, n=10 mice per group, data not shown). Consistent with previous reports (3), antagomiR-122 treatment resulted in a reduction of total cholesterol levels (Fig. 2*C*). Gene expression in the liver was down-regulated in the liver for ATP citrate lyase (*Acly*), microsomal triglyceride transfer protein (*Mttp*), and sterol regulatory element-binding protein 1 (*Srebp1*) (Fig. 2*D*).

At the protein level, we analysed consequences of antagomiR-122 treatment using both a label-free and a TMT-labelling approach (Fig. 2*E* and Supplementary Tables 1 & 2). Eleven proteins were returned as differentially expressed in both datasets and included proteins with an apparent connection to lipid metabolism, i.e. carnitine O-

palmitoyltransferase 1 (CPT1A), prolow-density lipoprotein receptor-related protein 1 (LRP1), and histidine triad nucleotide-binding protein 1 (HINT1). Few are predicted miR-122 targets (Supplementary Table 3), and the proteomics changes were not accompanied by corresponding changes in gene expression (Supplementary Fig. 3*A*). However, we observed a modest but significant downregulation of the GTPase Rab27a (Supplementary Fig. 3*B*), a key regulator of exosome release (24).

Effect of Statin Therapy on miR-122 Levels

We next assessed the effect of statin treatment on miR-122 levels. In the placebo-controlled clinical HACVD-ASCOT trial, 12-month atorvastatin treatment led not only to the expected reduction in total cholesterol and low-density lipoprotein cholesterol but also to a marked reduction in serum miR-122 levels (all $P<0.001$; Fig. 3*A*). In contrast, other miRNAs quantified in the same samples remained unchanged (data not shown).

In mice, atorvastatin treatment had only modest effects on hepatic miR-122 expression (+23%, $P=0.038$), but reduced serum miR-122 levels (-61%, $P=0.082$; Fig. 3*B*). Short-term treatment with statins in mice did not result in a reduction of total cholesterol levels (data not shown), which is in agreement with previous reports (25). Similarly, in murine primary hepatocytes, increasing doses of atorvastatin did not affect cellular miR-122 levels ($P_{trend}=0.575$), but markedly reduced miR-122 in the culture medium ($P_{trend}<0.001$; Fig. 3*C*). Thus, the inhibitory effect of atorvastatin on circulating miR-122 is independent of lipid levels and hepatic miR-122 expression.

Association of miR-122 with Development of new-onset Metabolic syndrome and T2DM

Among participants of the Bruneck free of pre-existing disease at baseline, we recorded new-onset of 136 events of metabolic syndrome and 57 events of T2DM. Age and sex-adjusted

risk ratios comparing top vs. bottom third of miR-122 levels were: 2.85 (1.78-4.56; *P*<0.001) for metabolic syndrome and 2.92 (1.34-6.35; *P*=0.007) for T2DM (Fig. 4). Age- and sex-adjusted risk ratios per 1-SD higher log miR-122 were 1.59 (1.30-1.95; *P*<0.001) for metabolic syndrome and 1.39 (1.05-1.84; *P*=0.021) for T2DM. Risk ratios were virtually identical when further adjusted for socioeconomic status, smoking, physical activity, and alcohol consumption: 1.60 (1.30-1.96; *P*<0.001) for metabolic syndrome and 1.37 (1.03-1.82; *P*=0.029). Risk ratios were somewhat attenuated upon further adjustment for body mass index and waist-hip ratio or for ln HOMA-IR. Results were broadly similar for women and men, and in subgroups according to statin intake and clinical categories of adiposity (Supplementary Fig. 4). miR-122 was not significantly associated with new-onset CVD events in the overall study (RR=1.10; 0.90-1.33; *P*=0.350), although subgroup analyses indicated a possibly stronger and significant association in participants aged <60 years compared to participants aged ≥60 years (*P* for interaction=0.006) (Supplementary Fig. 5).

DISCUSSION

In the present study, we use a multi-dimensional 'omics approach in a population-based study to identify metabolic signatures associated with miR-122. We report a number of important and entirely novel results based on miRNA measurements in >2000 human blood samples (from the 1995 and 2000 evaluations in the Bruneck Study plus ASCOT) combined with experimental follow-up to provide a mechanistic context as summarised in Fig. 5.

First, circulating miR-122 levels are elevated in people with prevalent metabolic syndrome or T2DM and correlate strongly with lipid subspecies containing saturated and monounsaturated fatty acids. In a prospective setting, elevated serum levels of miR-122 antedate the manifestation of metabolic syndrome and T2DM, but not CVD. Second, serum levels of miR-122 positively correlate with major lipids (triglycerides, LDL- and HDL-C) in

the general community and substantially decline with cholesterol-lowering statin therapy (atorvastatin 10 mg). We further corroborate this observation by *in vitro* and *in vivo* experiments demonstrating a reduction of miR-122 in the supernatant of atorvastatin-treated murine hepatocytes and in serum of atorvastatin-treated wild-type mice and confirmed miR-122 effects on enzymes involved in lipid metabolism in the liver. Overall, we provide strong evidence for circulating miR-122 being a marker of hepatic lipid metabolism.

System-wide Relations of Circulating miR-122

MiR-122, which is primarily expressed in the liver, has been suggested to regulate the expression of various genes associated with cholesterol and fatty acid metabolism (2). In mice, inhibition of miR-122 led to markedly lower plasma cholesterol levels, halted hepatic lipid synthesis, and enhanced hepatic fatty acid oxidation (4,5). Two studies in non-human primates reported similar reductions in cholesterol (6,7).

In line with these reports, our study showed that inhibition of miR-122 in mice using antagomiR-122 led to a down-regulated expression of genes implicated in lipid metabolism (Fig. 2*D*), such as ATP citrate lyase (*Acly*), microsomal triglyceride transfer protein (*Mttp*), and sterol regulatory element-binding protein 1 (*Srebp-1*) (26). This is further corroborated by the notion that miR-122 knockout mice express less *Mttp*, an essential enzyme that regulates the assembly of lipoproteins (27,28). Furthermore, our proteomic analysis of liver extracts from antagomiR-122-treated mice (Fig. 2*E*) revealed increases in carnitine O-palmitoyltransferase 1 (CPT1A), a rate-limiting enzyme of fatty acid oxidation, that was not observed at the gene expression level (Fig. 2*D*, CPT1), and prolow-density lipoprotein receptor-related protein 1 (LRP1), which plays a key role in cholesterol biosynthesis (29), HDL secretion from hepatocytes (30), and the removal of atherogenic lipoproteins, including VLDL (31). The proteomic analysis also identified a decrease in histidine triad nucleotide-

binding protein 1 (HINT1), which – based on data from *Hint-1*-deficient mice – is expected to contribute to reductions of total and esterified cholesterol (32).

These data provide mechanistic underpinning for our observation in the Bruneck Study that circulating miR-122 levels are positively associated with lipid subspecies that can be produced by hepatic *de novo* lipogenesis (Fig. 1*A*). We and others have previously shown that these lipid subspecies, comprised of saturated and monounsaturated fatty acids, are associated with a higher risk of CVD (9) and T2DM (33). We also identified strong positive correlations with apolipoproteins found on VLDL (apoB100, apoC1, apoC2, apoE), and inverse correlations with plasma apoD (present mainly in HDL) and apoA4 (a major component of HDL and chylomicrons) (Fig. 1*B*). Moreover, our comprehensive assessment of plasma proteins returned a positive correlation with afamin, which was previously linked to prevalent and new-onset metabolic syndrome and all its components (34), a positive correlation with complement factor H, a protein that binds malondialdehyde epitopes and protects from oxidative stress (35), and an inverse correlation with zinc-alpha-2-glycoprotein, an adipokine that leads to lipid degradation and higher insulin sensitivity in adipocytes (36,37).

Circulating miR-122 as Novel Biomarker

In the current study, we show – for the first time – that baseline levels of miR-122 are associated with development of metabolic syndrome and with T2DM (Fig. 4). Notably, associations did not vary by degree of adiposity, a strong determinant of cardiometabolic risk (38,39). Statin treatment decreased both lipoprotein and miR-122 release from the liver. Since miR-122 is either absent from lipoproteins, including VLDL and HDL (Supplementary Table 4), or only present at very low levels, i.e. in LDL (40), the pronounced effect of statins on circulating miR-122 levels cannot be explained by effects on plasma lipoproteins. Instead,

it is probably caused by reduced secretion of liver exosomes (Fig. 5), in which miR-122 has been localized in abundance (41,42). Circulating miR-122 is undetectable in exosome-depleted serum (42). By inhibiting cholesterol synthesis, statins also modulate protein prenylation (43). This posttranslational modification promotes the membrane localisation of proteins, in particular of Rab27 proteins that control the different steps of exosome secretion (24,44). Statins may reduce circulating miR-122 levels by inhibiting the prenylation of Rab proteins and hepatic exosome secretion. The latter might constitute a novel part of the beneficial pleiotropic effects of statins. This is further corroborated by our findings in mice, demonstrating a reduction of circulating miR-122 levels after short-term treatment with atorvastatin without concomitant reduction in total cholesterol levels and reduced gene expression of Rab27a in response to antagomiR-122 treatment, the key effector GTPase that drives the exosome-release process (Supplementary Fig. 3*B*).

Strengths and Limitations

The prospective Bruneck cohort is extremely well-characterized with a 100% follow-up and high-quality ascertainment of clinical endpoints and potential confounders. MiR-122 was measured in serum and plasma. We incorporated repeat measurements of miR-122 in our statistical models, which is particularly important given that the within-person variability of miR-122 was high (correlation coefficient over 5 years: 0.24). In contrast to platelet-related miRNAs, which are reduced in diabetic patients (21,45), miR-122 levels showed positive associations with metabolic syndrome and T2DM and were highly correlated in serum and plasma. Expression data in the human liver would be a more direct measure, but, clearly, this is not feasible in population studies. The Bruneck Study was conducted in an entirely Caucasian population. Thus, it remains to be determined whether these findings equally apply to other ethnicities.

Conclusions

High circulating miR-122 levels correlate with complex lipids containing saturated and monounsaturated fatty acids that can be derived from hepatic *de novo* lipogenesis and an adverse metabolic profile. Inhibition of HMG-CoA reductase by atorvastatin reduces miR-122 release. Circulating miR-122 levels are associated with future development of metabolic syndrome and T2DM in the general population.

Funding. P.W. was supported by an Erwin-Schrödinger-Fellowship sponsored by the Austrian Science Fund (J-3679-B13). A.Z. and M.M. are Intermediate and Senior Fellows of the British Heart Foundation (FS/13/18/30207 and FS/13/2/29892, respectively). The study was supported by a British Heart Foundation special project grant (SP/12/5/29574), the Fondation Leducq (MIRVAD; 13 CVD 02), Diabetes UK (12/0004530), and an excellence initiative (Competence Centers for Excellent Technologies – COMET) of the Austrian Research Promotion Agency FFG: "Research Center of Excellence in Vascular Ageing – Tyrol, VASCage" (K-Project number 843536). The Bruneck Study was supported by the 'Pustertaler Verein zur Prävention von Herz- und Hirngefaesserkrankungen, Gesundheitsbezirk Bruneck' and the 'Assessorat für Gesundheit', Province of Bolzano, Italy. The HACVD study was supported by an investigational grant from Pfizer International, New York, NY, USA. The principal funding source for ASCOT was Pfizer, New York, NY, USA. Servier Research Group, Paris, France, and Leo Laboratories, Copenhagen, Denmark provided additional funding. D.K. was supported by a scholarship sponsored by the "Studienstiftung des deutschen Volkes". C.M.R. was supported by a grant from American Heart Association (15SDG23000025). A.H. was supported by the National Institute for Health Research University College London Hospitals Biomedical Research Centre. This work was also supported by JDRF and the NIHR Biomedical Research Center based at Guy's and St Thomas' National Health Service Foundation Trust and King's College London in partnership with King's College Hospital. This work was also supported by grants from the NIH (R01HL107953, and R01HL106063 to C.F.H.; 1F31AG043318 to L.G.) and the Foundation Leducq Transatlantic Network of Excellence in Cardiovascular Research (to M.M. and C.F.H.).

Duality of Interest. The Medical University of Innsbruck and King's College London filed patent applications on miRNA biomarkers.

Author Contributions. P.W., P.Skroblin, X.Y., D.K., A.Z., A.L.M., C.M.R., L.G., N.R., E.B., A.D.H., P.Santer, C.F.H., H.T., J.W., S.K., and M.M. researched data. P.W., X.Y., and S.K. analyzed data. P.W., P.Skroblin, S.K., and M.M. interpreted data. P.W., S.K., and M.M. wrote the manuscript. P.Skroblin, X.Y., D.K., A.Z., A.L.M., C.M.R., L.G., N.R., E.B., A.D.H., P. Santer, C.F.H., H.T., and J.W. reviewed and edited the manuscript. P.W. is the guarantor of this work and, as such, had full access to all the data in the study and takes responsibility for the integrity of the data and the accuracy of the data analysis.

REFERENCES

1. Bartel DP. MicroRNAs: target recognition and regulatory functions. Cell 2009;136:215–233.
2. Fernández-Hernando C, Ramírez CM, Goedeke L, Suárez Y. MicroRNAs in metabolic disease. Arterioscler Thromb Vasc Biol 2013;33:178–185.
3. Willeit P, Skroblin P, Kiechl S, Fernández-Hernando C, Mayr M. Liver microRNAs: potential mediators and biomarkers for metabolic and cardiovascular disease? Eur Heart J 2016; Epub ahead of print.
4. Esau C, Davis S, Murray SF, et al. miR-122 regulation of lipid metabolism revealed by in vivo antisense targeting. Cell Metab 2006;3:87–98.
5. Krützfeldt J, Rajewsky N, Braich R, et al. Silencing of microRNAs in vivo with 'antagomirs'. Nature 2005;438:685–689.
6. Elmén J, Lindow M, Schütz S, et al. LNA-mediated microRNA silencing in non-human primates. Nature 2008;452:896–899.
7. Lanford RE, Hildebrandt-Eriksen ES, Petri A, et al. Therapeutic silencing of microRNA-122 in primates with chronic hepatitis C virus infection. Science 2010;327:198–201.
8. Gao W, He HW, Wang ZM, et al. Plasma levels of lipometabolism-related miR-122 and miR-370 are increased in patients with hyperlipidemia and associated with coronary artery disease. Lipids Health Dis 2012;11:55.
9. Stegemann C, Pechlaner R, Willeit P, et al. Lipidomics profiling and risk of cardiovascular disease in the prospective population-based bruneck study. Circulation 2014;129:1821–1831.
10. Willeit P, Kiechl S, Kronenberg F, et al. Discrimination and net reclassification of cardiovascular risk with lipoprotein(a): prospective 15-year outcomes in the Bruneck Study. J Am Coll Cardiol 2014;64:851–860.
11. Zampetaki A, Willeit P, Tilling L, et al. Prospective study on circulating MicroRNAs and risk of myocardial infarction. J Am Coll Cardiol 2012;60:290–299.
12. Kiechl S, Wittmann J, Giaccari A, et al. Blockade of receptor activator of nuclear factor-κB (RANKL) signaling improves hepatic insulin resistance and prevents development of diabetes mellitus. Nat Med 2013;19:358–63.
13. Willeit P, Willeit J, Brandstätter A, et al. Cellular aging reflected by leukocyte telomere length predicts advanced atherosclerosis and cardiovascular disease risk. Arterioscler Thromb Vasc Biol 2010;30:1649–1656.
14. Baecke JA, Burema J, Frijters JE. A short questionnaire for the measurement of habitual physical activity in epidemiological studies. Am J Clin Nutr 1982;36:936–942.
15. Bonora E, Kiechl S, Willeit J, et al. Metabolic syndrome: epidemiology and more extensive phenotypic description. Cross-sectional data from the Bruneck Study. Int J Obes Relat Metab Disord 2003;27:1283–1289.
16. Sever PS, Dahlöf B, Poulter NR, et al. Prevention of coronary and stroke events with atorvastatin in hypertensive patients who have average or lower-than-average cholesterol concentrations, in the Anglo-Scandinavian Cardiac Outcomes Trial–Lipid Lowering Arm (ASCOT-LLA): a multicentre randomised controlled trial. Lancet 2003;361:1149–1158.
17. Poulter NR, Wedel H, Dahlöf B, et al. Role of blood pressure and other variables in the differential cardiovascular event rates noted in the Anglo-Scandinavian Cardiac Outcomes Trial-Blood Pressure Lowering Arm (ASCOT-BPLA). Lancet 2005;366:907–913.

18. Stanton A, Fitzgerald D, Hughes A, et al. An intensive phenotyping study to enable the future examination of genetic influences on hypertension-associated cardiovascular disease. J Hum Hypertens 2001;15 Suppl 1:S13–S18.
19. Zampetaki A, Attia R, Mayr U, et al. Role of miR-195 in aortic aneurysmal disease. Circ Res 2014;115:857–866.
20. Werner T, Sweetman G, Savitski MF, Mathieson T, Bantscheff M, Savitski MM. Ion coalescence of neutron encoded TMT 10-plex reporter ions. Anal Chem 2014;86:3594–3601.
21. Willeit P, Zampetaki A, Dudek K, et al. Circulating microRNAs as novel biomarkers for platelet activation. Circ Res 2013;112:595–600.
22. D'Agostino RB, Lee ML, Belanger AJ, Cupples LA, Anderson K, Kannel WB. Relation of pooled logistic regression to time dependent Cox regression analysis: the Framingham Heart Study. Stat Med 1990;9:1501–1515.
23. Bertoia ML, Bertrand KA, Sawyer SJ, Rimm EB, Mukamal KJ. Reproducibility of Circulating MicroRNAs in Stored Plasma Samples. PLoS One 2015;10:e0136665.
24. Ostrowski M, Carmo NB, Krumeich S, et al. Rab27a and Rab27b control different steps of the exosome secretion pathway. Nat Cell Biol 2010;12:19–30; sup pp 1–13.
25. Schonewille M, Freark de Boer J, Mele L, et al. Statins increase hepatic cholesterol synthesis and stimulate fecal cholesterol elimination in mice. J Lipid Res 2016;57:1455–1464.
26. Menon B, Sinden J, Franzo-Romain M, Botta RB, Menon KMJ. Regulation of LH receptor mRNA binding protein by miR-122 in rat ovaries. Endocrinology 2013;154:4826–4834.
27. Wen J, Friedman JR. miR-122 regulates hepatic lipid metabolism and tumor suppression. J Clin Invest 2012;122:2773–2776.
28. Tsai WC, Hsu SD, Hsu CS, et al. MicroRNA-122 plays a critical role in liver homeostasis and hepatocarcinogenesis. J Clin Invest 2012;122:2884–2897.
29. El Asmar Z, Terrand J, Jenty M, et al. Convergent Signaling Pathways Controlled by LRP1 (Receptor-related Protein 1) Cytoplasmic and Extracellular Domains Limit Cellular Cholesterol Accumulation. J Biol Chem 2016;291:5116–5127.
30. Basford JE, Wancata L, Hofmann SM, et al. Hepatic deficiency of low density lipoprotein receptor-related protein-1 reduces high density lipoprotein secretion and plasma levels in mice. J Biol Chem 2011;286:13079–13087.
31. Medh JD, Bowen SL, Fry GL, et al. Hepatic triglyceride lipase promotes low density lipoprotein receptor-mediated catabolism of very low density lipoproteins in vitro. J Lipid Res 1999;40:1263–1275.
32. Beyo?lu D, Krausz KW, Martin J, et al. Disruption of tumor suppressor gene Hint1 leads to remodeling of the lipid metabolic phenotype of mouse liver. J Lipid Res 2014;55:2309–2319.
33. Rhee EP, Cheng S, Larson MG, et al. Lipid profiling identifies a triacylglycerol signature of insulin resistance and improves diabetes prediction in humans. J Clin Invest 2011;121:1402–1411.
34. Kronenberg F, Kollerits B, Kiechl S, et al. Plasma concentrations of afamin are associated with the prevalence and development of metabolic syndrome. Circ Cardiovasc Genet 2014;7:822–829.
35. Weismann D, Hartvigsen K, Lauer N, et al. Complement factor H binds malondialdehyde epitopes and protects from oxidative stress. Nature 2011;478:76–81.

36. Garrido-Sánchez L, García-Fuentes E, Fernández-García D, et al. Zinc-alpha 2-glycoprotein gene expression in adipose tissue is related with insulin resistance and lipolytic genes in morbidly obese patients. PLoS One 2012;7:e33264.
37. Yang M, Liu R, Li S, et al. Zinc-α2-glycoprotein is associated with insulin resistance in humans and is regulated by hyperglycemia, hyperinsulinemia, or liraglutide administration: cross-sectional and interventional studies in normal subjects, insulin-resistant subjects, and subjects with newly diagnosed diabetes. Diabetes Care 2013;36:1074–1082.
38. Würtz P, Wang Q, Kangas AJ, et al. Metabolic signatures of adiposity in young adults: Mendelian randomization analysis and effects of weight change. PLoS Med 2014;11:e1001765.
39. Fall T, Hägg S, Mägi R, et al. The role of adiposity in cardiometabolic traits: a Mendelian randomization analysis. PLoS Med 2013;10:e1001474.
40. Vickers KC, Palmisano BT, Shoucri BM, Shamburek RD, Remaley AT. MicroRNAs are transported in plasma and delivered to recipient cells by high-density lipoproteins. Nat Cell Biol 2011;13:423–433.
41. Huang X, Yuan T, Tschannen M, et al. Characterization of human plasma-derived exosomal RNAs by deep sequencing. BMC Genomics 2013;14:319.
42. Gallo A, Tandon M, Alevizos I, Illei GG. The majority of microRNAs detectable in serum and saliva is concentrated in exosomes. PLoS One 2012;7:e30679.
43. Wang CY, Liu PY, Liao JK. Pleiotropic effects of statin therapy: molecular mechanisms and clinical results. Trends Mol Med 2008;14:37–44.
44. Jaé N, McEwan DG, Manavski Y, Boon RA, Dimmeler S. Rab7a and Rab27b control secretion of endothelial microRNA through extracellular vesicles. FEBS Lett 2015;589:3182–3188.
45. Elgheznawy A, Shi L, Hu J, et al. Dicer cleavage by calpain determines platelet microRNA levels and function in diabetes. Circ Res 2015;117:157–165.

TABLES

Table 1 – Baseline characteristics and cross-sectional correlates of miR-122 in the Bruneck Study.

Variable	Mean (SD) or n (%)	Age- and sex-adjusted difference in miR-122 per SD or compared to reference (95% CI)*	P value
Questionnaire-based			
Age, years	63 (11)	-3% (-19, 17%)	0.753
Female sex, n (%)	405 (50%)	+31% (-10, 89%)	0.153
Current smoker, n (%)	159 (20%)	-22% (-51, 26%)	0.314
Physical activity, Baeke score	2.3 (0.9)	+1% (-18, 24%)	0.932
Alcohol consumption, g/d	24 (31)	-1% (-21, 23%)	0.919
Statin treatment, n (%)	26 (3%)	-12% (-69, 151%)	0.808
Socioeconomic status			
Low, n (%)	494 (61%)	[Reference]	
Middle, n (%)	176 (22%)	-30% (-56, 14%)	0.150
High, n (%)	140 (17%)	+65% (-2, 177%)	0.058
Liver enzymes			
Alanine transaminase, U/l	23 (13)	+112% (76, 155%)	**<0.001**
Aspartate aminotransferase, U/l	24 (9.3)	+81% (51, 118%)	**<0.001**
Adiposity measures			
Body mass index, kg/m^2	26 (3.9)	+41% (17, 69%)	**<0.001**
Waist-hip ratio	0.93 (0.072)	+44% (17, 76%)	**<0.001**
Markers of inflammation			
Log hsCRP, mg/l	-1.7 (1.0)	+42% (17, 71%)	**<0.001**
Markers of dysglycaemia			
Fasting plasma glucose, mg/dl	102 (25)	+23% (2, 48%)	0.030
HbA1c, % [mmol/mol]	5.6 (1.8) [38 (20)]	+4% (-14, 25%)	0.704
Log HOMA-IR	1.1 (0.6)	+67% (39, 101%)	**<0.001**
Major lipids			
Total cholesterol, mg/dl	230 (43)	+19% (-1, 43%)	0.070
LDL cholesterol, mg/dl	145 (38)	+21% (1, 46%)	0.043
HDL cholesterol, mg/dl	59 (16)	-34% (-45, -21%)	**<0.001**
Log triglycerides, mg/dl	4.8 (0.5)	+62% (35, 94%)	**<0.001**

FIGURE LEGENDS

Figure 1 – Cross-sectional correlation of serum miR-122 levels with lipid subspecies (Panel A) and selected proteins related to lipid metabolism (Panel B) in the Bruneck Study. In Panel A, lipid species are arranged by lipid class in 8 panels according to the number of total carbon atoms and number of double bonds. Lipid species highlighted with a yellow halo showed statistically significant correlations after Bonferroni-correction. For better visibility, those lipid species with alkyl ether linkage are shifted upwards, whereas their alkyl-ether-free counterparts are shifted downward. In Panel B, P values significant after Bonferroni-correction are shown in bold. The full panel of proteins are shown in Supplementary Figure 2. Abbreviations: AFAM, afamin; CE, cholesteryl ester; CFAH, complement factor H; LPC, lysophosphatidylcholine; LPE, lysophosphatidylethanolamine; PC, phosphatidylcholine; PE, phosphatidylethanolamine; PS, phosphatidylserine; SM, sphingomyelin; TAG, triacylglycerol; and ZA2G, zinc-alpha-2-glycoprotein.

Figure 2 – Effects of antagomiR-122 injection in mice. Liver miR-122 expression was assessed by Northern blotting (Panel A); expression of other hepatic miRNAs involved in lipoprotein metabolism (Panel B); serum cholesterol (Panel C); gene expression (Panel D); and hepatic proteome profile (Panel E). Two proteomics methods were used for quantitation: a label-free method based on spectral counting and a 10-plex experiment using TMT labelling. Proteins that were returned as differentially expressed by both techniques are highlighted (for details, see Supplementary Tables 1 & 2). Abbreviations: *Acc1*, acetyl-CoA carboxylase; *Acly*, ATP citrate lyase; *Aldo*, aldolase; *Ampk*, 5' AMP-activated protein kinase; CP2AC, cytochrome P450 2A12; *Cpt1*, carnitine palmitoyltransferase 1; CPT1A, liver isoform of carnitine O-palmitoyltransferase 1; *Fasn*, fatty acid synthase; GRN, granulins;

HINT1, histidine triad nucleotide-binding protein 1; *Hmgcr*, HMG-CoA reductase; *Ldlr*, LDL receptor; LRP1, prolow-density lipoprotein receptor-related protein 1; *Mttp*, microsomal triglyceride transfer protein; RL23A, 60S ribosomal protein L23a; RL37A, 60S ribosomal protein L37a; RS16, 40S ribosomal protein S16; RS18, 40S ribosomal protein S18; *Scd1*, Stearoyl-CoA desaturase-1; and *Srebp*, sterol regulatory element-binding protein.

Figure 3 – Effects of atorvastatin treatment on total cholesterol, LDL cholesterol (Panel A), and serum miR-122 in ASCOT participants (Panel B), serum miR-122 in mice (Panel C), and miR-122 secretion from primary hepatocytes (Panel D).

Figure 4 – Association of miR-122 with new-onset metabolic syndrome and T2DM in the Bruneck Study. *Age, sex, socio-economic status, smoking, physical activity, and alcohol consumption. Asterisks indicate level of significance: *P<0.05; **P<0.01; ***P<0.001.

Figure 5 – Summary of the key findings.

(A)

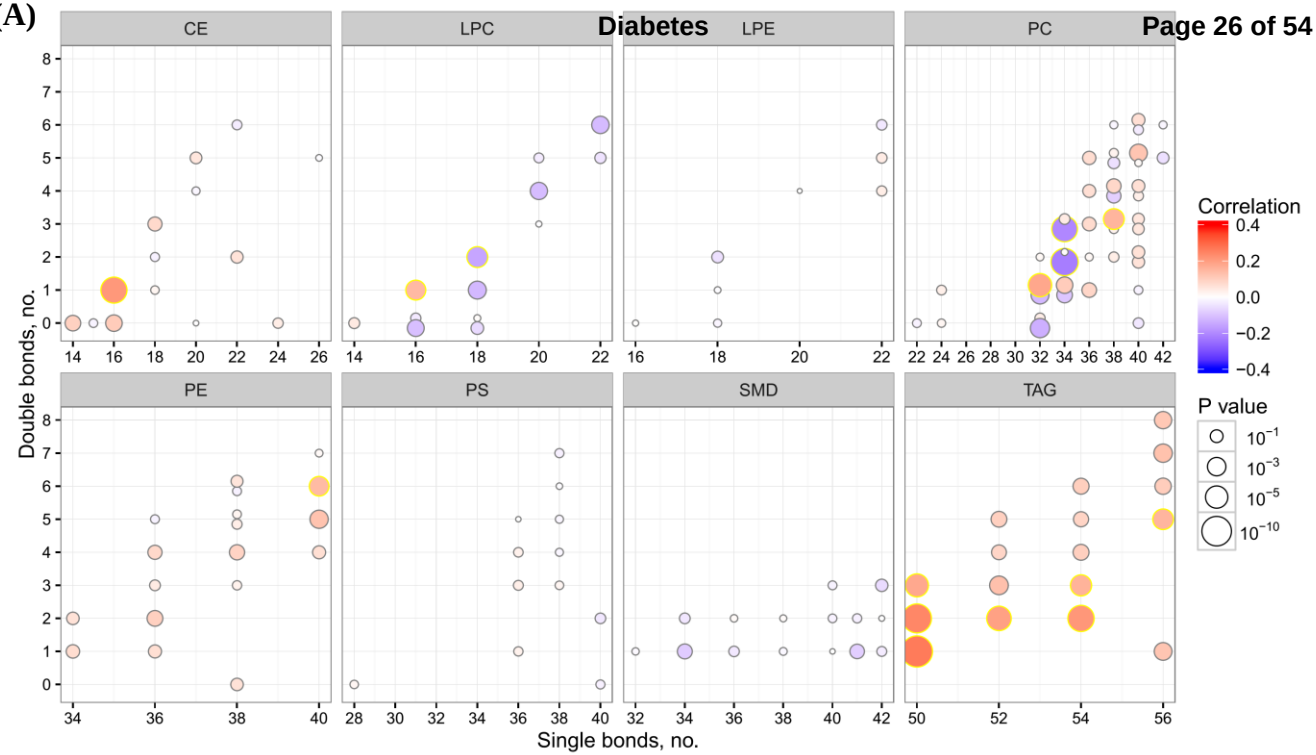

(B)

Protein	Age- and sex-adjusted Spearman correlation coefficient (95% CI) between protein and circulating miR-122	P value
Apolipoproteins		
APOA1	-0.04 (-0.12, 0.03)	0.262
APOA2	0.11 (0.03, 0.18)	0.007
APOA4	-0.16 (-0.23, -0.09)	**3×10^{-5}**
APOB	0.17 (0.10, 0.25)	**6×10^{-6}**
APOC1	0.03 (-0.05, 0.10)	0.510
APOC2	0.21 (0.13, 0.28)	**6×10^{-8}**
APOC3	0.17 (0.10, 0.24)	**8×10^{-6}**
APOD	-0.16 (-0.23, -0.08)	**4×10^{-5}**
APOE	0.19 (0.11, 0.26)	**1×10^{-6}**
APOH	0.06 (-0.01, 0.14)	0.113
APOL1	0.14 (0.06, 0.21)	**4×10^{-4}**
APOM	-0.02 (-0.09, 0.06)	0.626
Other proteins		
AFAM	0.42 (0.36, 0.48)	**4×10^{-30}**
CFAH	0.21 (0.14, 0.28)	**3×10^{-8}**
ZA2G	-0.28 (-0.35, -0.21)	**1×10^{-13}**

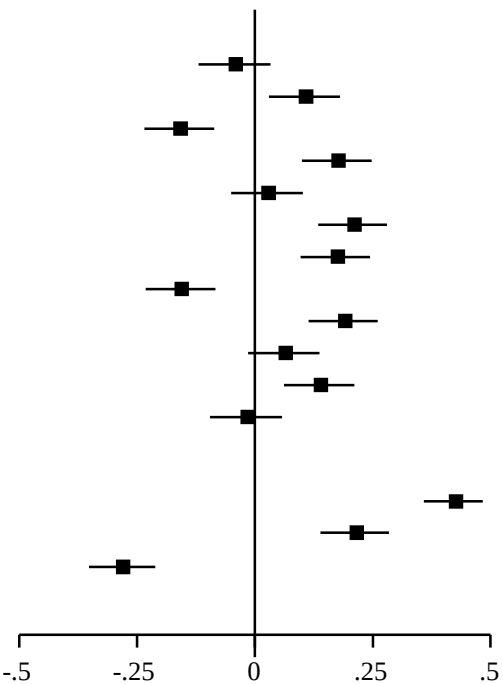

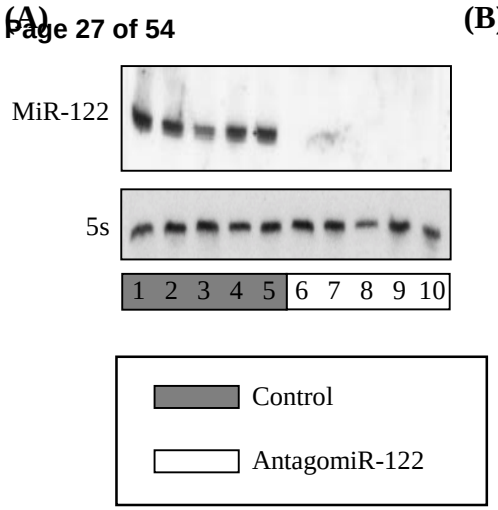
(A)
MiR-122
5s
1 2 3 4 5 6 7 8 9 10
Control
AntagomiR-122

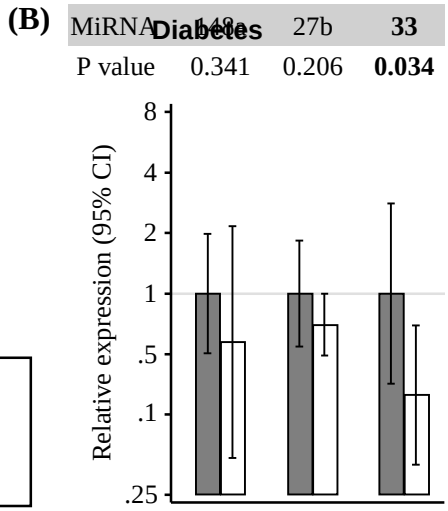
(B)
MiRNA Diabetes
P value
148a 0.341
27b 0.206
33 0.034
Relative expression (95% CI)
8
4
2
1
.5
.1
.25

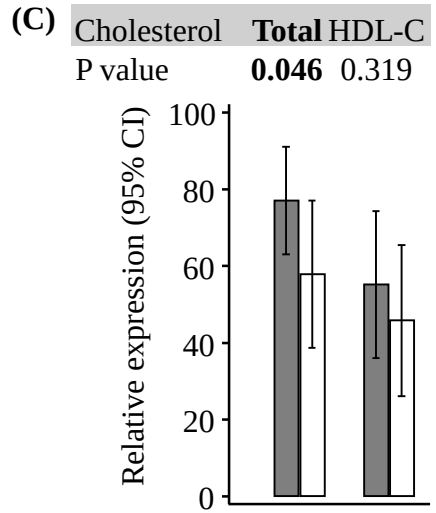
(C)
Cholesterol Total HDL-C
P value
0.046 0.319
Relative expression (95% CI)
100
80
60
40
20
0

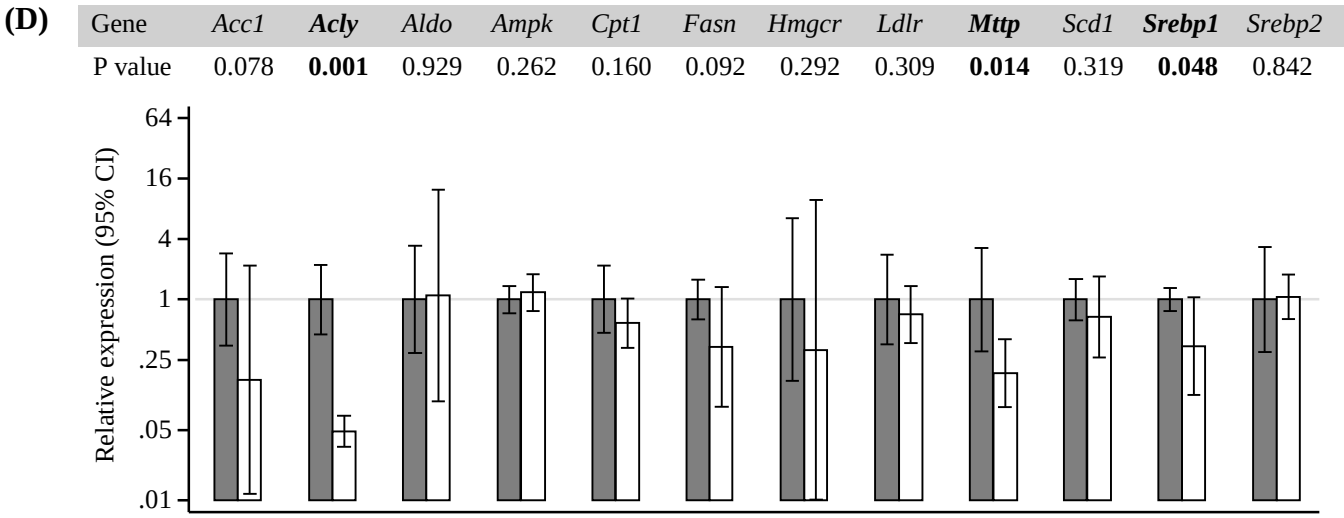
(D)
Gene Acc1 Acly Aldo Ampk Cpt1 Fasn Hmgcr Ldlr Mttp Scd1 Srebp1 Srebp2
P value 0.078 0.001 0.929 0.262 0.160 0.092 0.292 0.309 0.014 0.319 0.048 0.842
Relative expression (95% CI)
64
16
4
1
.25
.05
.01

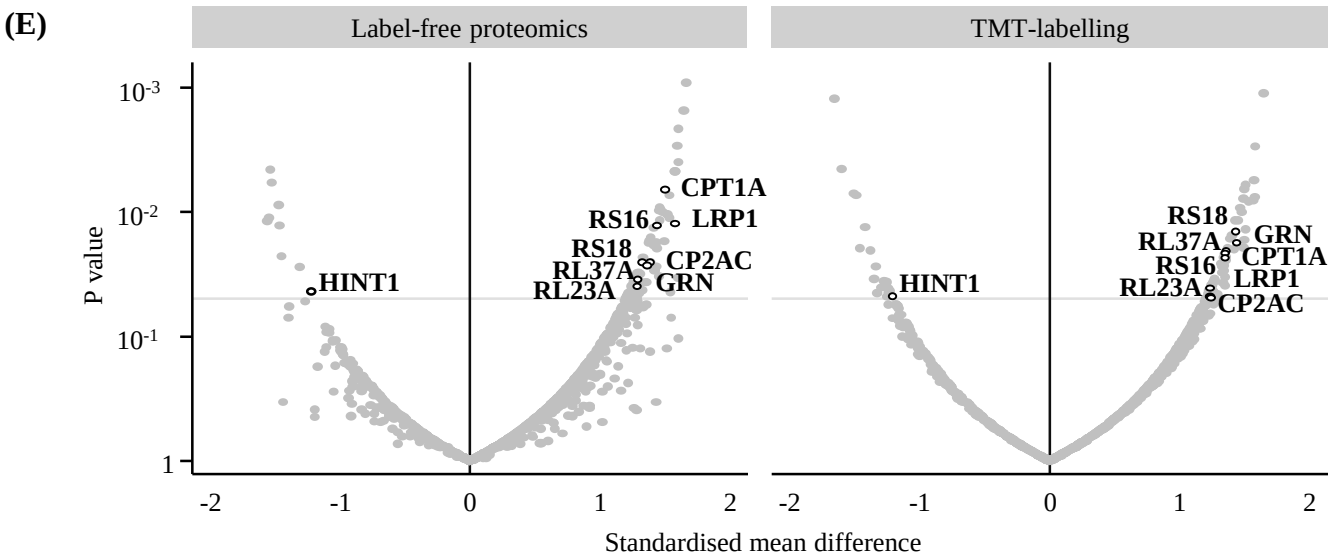
(E)
Label-free proteomics
TMT-labelling
P value
10-3
10-2
10-1
1
HINT1
CPT1A
RS16
LRP1
RS18
CP2AC
RL37A
GRN
RL23A
-2
-1
0
1
2
Standardised mean difference

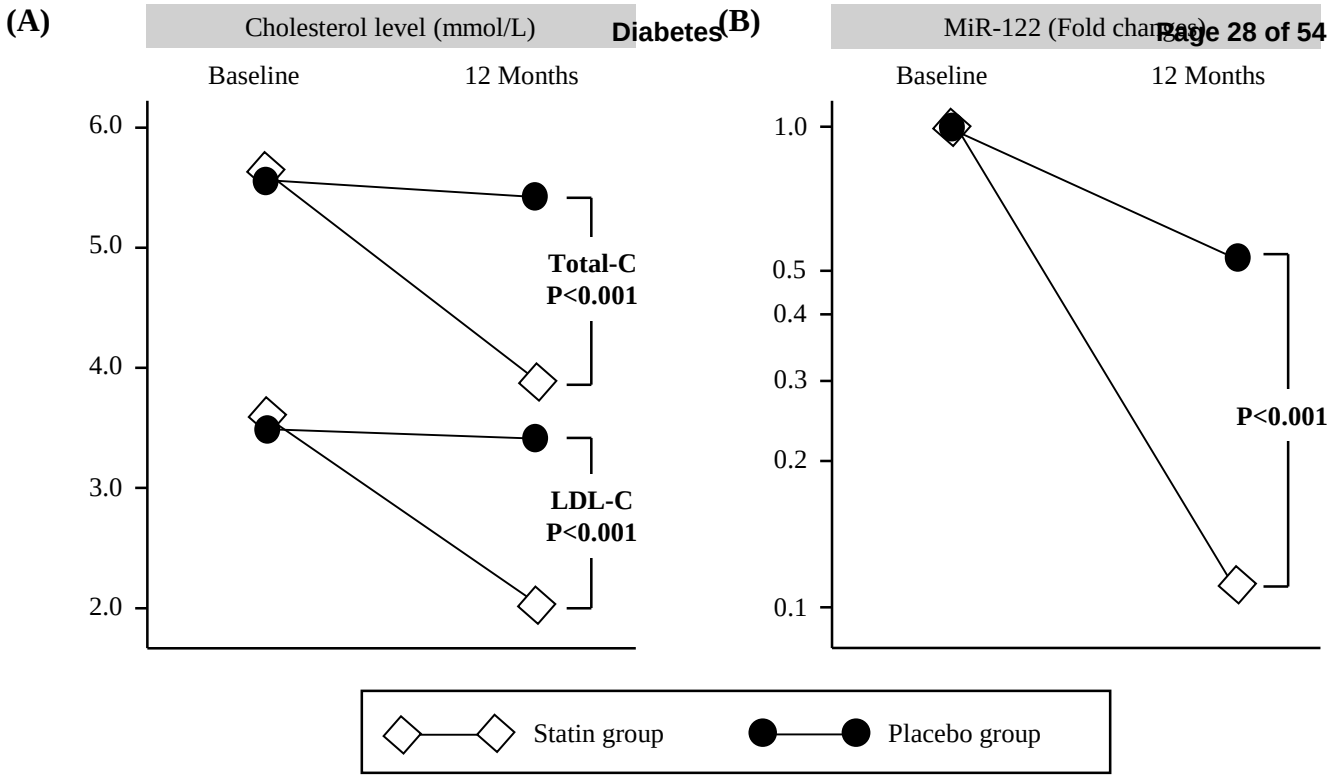
(A)
Cholesterol level (mmol/L)
Baseline
12 Months
6.0
5.0
4.0
3.0
2.0
Total-C
P<0.001
LDL-C
P<0.001
(B)
MiR-122 (Fold change)
Baseline
12 Months
1.0
0.5
0.4
0.3
0.2
0.1
P<0.001
Statin group
Placebo group

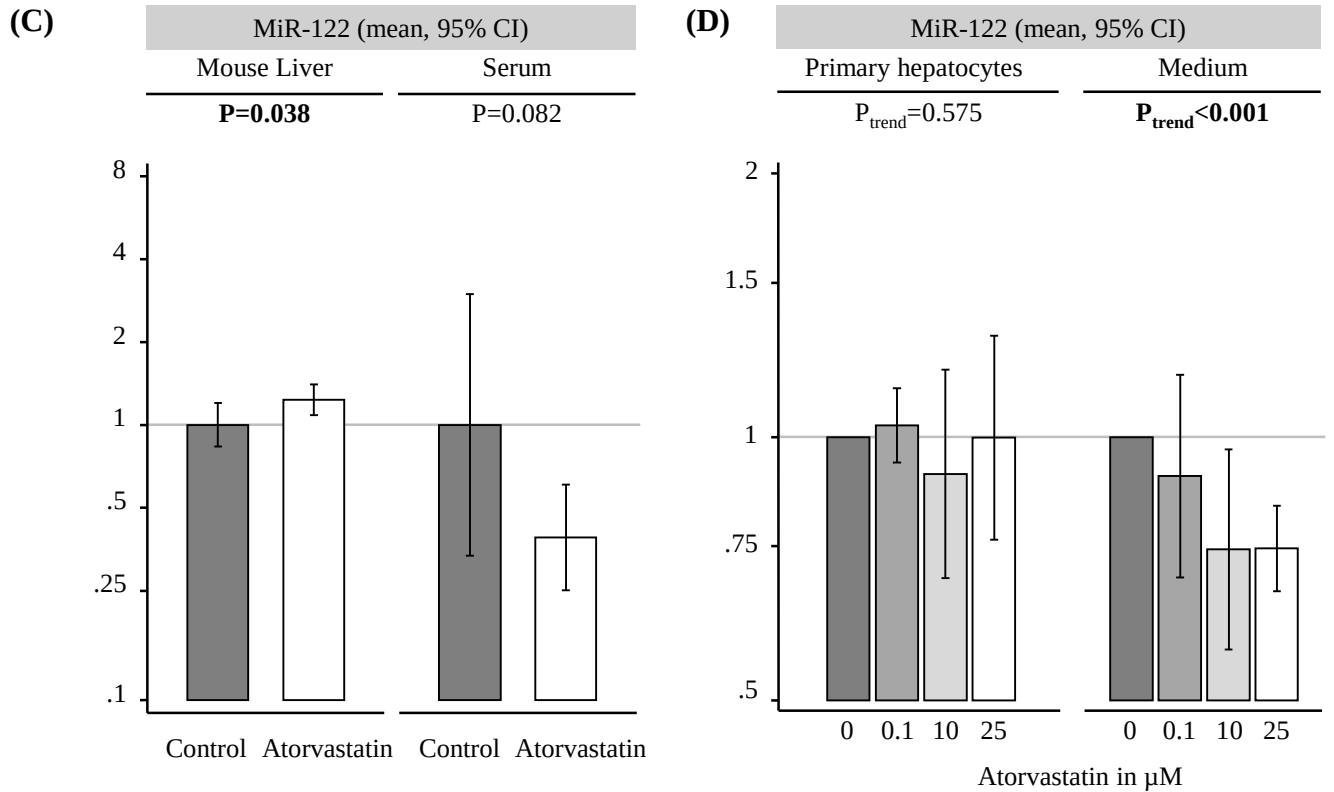
(C)
MiR-122 (mean, 95% CI)
Mouse Liver
Serum
P=0.038
P=0.082
8
4
2
1
.5
.25
.1
Control
Atorvastatin
Control
Atorvastatin
(D)
MiR-122 (mean, 95% CI)
Primary hepatocytes
Medium
P trend=0.575
P trend<0.001
2
1.5
1
.75
.5
0
0.1
10
25
0
0.1
10
25
Atorvastatin in µM

Outcome/ Level of adjustment	Top vs. bottom third of circulating miR-122		Per 1-SD higher circulating log miR-122	
	RR (95% CI)	P value	RR (95% CI)	P value
Metabolic syndrome (136 outcomes)				
Adjusted for age and sex	2.85 (1.78, 4.56)	**<0.001**	1.59 (1.30, 1.95)	**<0.001**
Multivariable model*	2.81 (1.76, 4.50)	**<0.001**	1.60 (1.30, 1.96)	**<0.001**
+ BMI + WHR	2.44 (1.48, 4.02)	**<0.001**	1.49 (1.19, 1.87)	**<0.001**
+ ln(HOMA-IR)	2.47 (1.53, 3.99)	**<0.001**	1.50 (1.22, 1.85)	**<0.001**
Type-2 diabetes (57 outcomes)				
Adjusted for age and sex	2.92 (1.34, 6.35)	**0.007**	1.39 (1.05, 1.84)	**0.021**
Multivariable model*	2.84 (1.30, 6.19)	**0.009**	1.37 (1.03, 1.82)	**0.029**
+ BMI + WHR	2.56 (1.16, 5.64)	**0.020**	1.31 (0.98, 1.76)	0.066
+ ln(HOMA-IR)	2.32 (1.05, 5.12)	0.037	1.26 (0.94, 1.70)	0.122

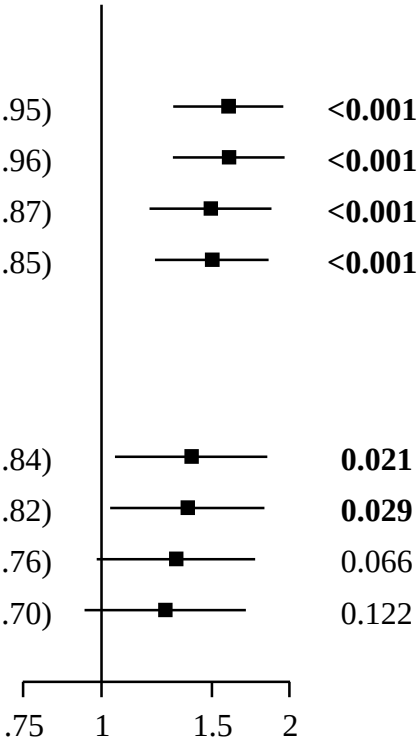

Correlates in humans

Correlation with clinical characteristics, 92 plasma proteins and 135 lipid species

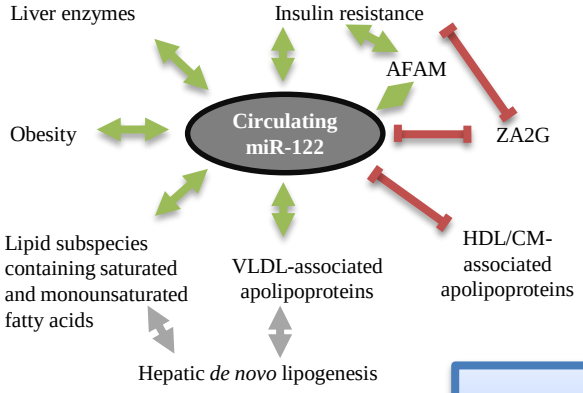

Inhibition with antagomir-122 in mice

Effects of miR-122 inhibition on gene expression and protein levels

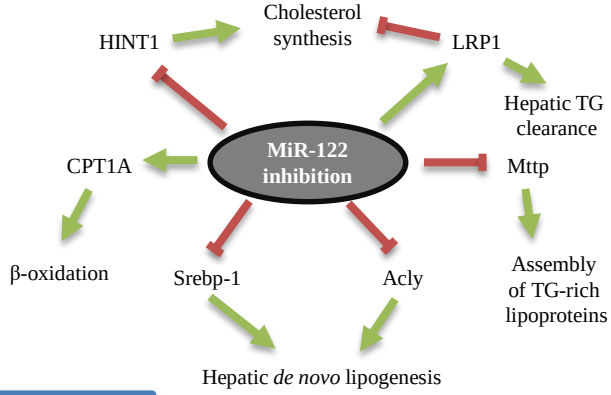

MicroRNA-122 and metabolic diseases

Statin intervention studies

MiR-122 ( ) localizes to hepatic exosomes ( ), not lipoproteins ( )

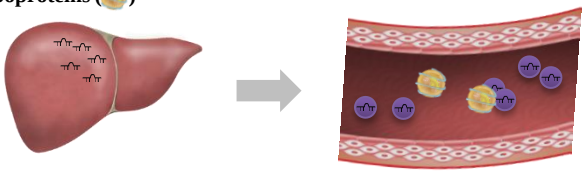

Studies in humans, mice and primary hepatocytes

Pleotropic effect of statins on exosome secretion

Association with disease risk

Development of new-onset disease over 15 years

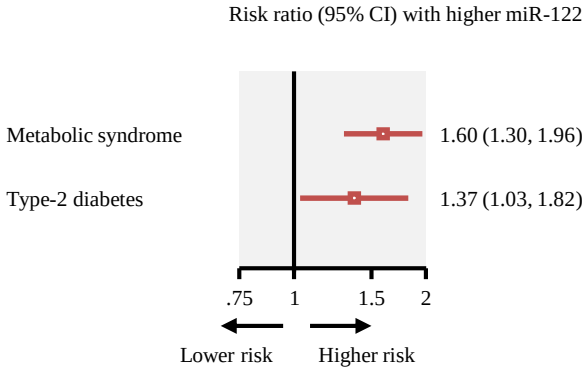

Positive correlation
Inverse correlation
Upregulation
Downregulation

Circulating MicroRNA-122 Is Associated With The Risk of New-Onset Metabolic Syndrome And Type-2-Diabetes

Online Appendix

Northern blot. Hepatic miRNA-122 expression was assessed by Northern blot analysis as previously described (1). Briefly, total RNA (5μg) was separated on a 15% acrylamide TBE 8M urea gel and blotted onto a Hybond N+ nylon filter (Amersham Biosciences). DNA oligonucleotides complementary to mature miR-122 (5'- AAACACCATTGTCACACTCCA-3') were end-labeled with [α-^{32}P] ATP and T_4 polynucleotide kinase (New England Biolabs) to generate high-specific activity probes. Hybridization was carried out according to the ExpressHyb (Clontech) protocol. Following overnight membrane hybridization with specific radiolabeled probes, membranes were washed once for 30min at 42°C in 4x SSC/0.5% SDS and subjected to autoradiography. Blots were re-probed for 5S rRNA (5′-CAGGCCCGACCCTGCTTAGCTTCCGAGAGATCAGACGAGAT-3′) to control for equal loading.

Quantitative real-time PCR (qRT-PCR). Total RNA was isolated from liver and murine hepatocyte samples using the Bullet Blender Homogenizer (Next Advance) in TRIzol reagent (Invitrogen) according to the manufacturer's protocol. For mRNA quantification, cDNA was synthesized using iScript RT Supermix (Bio-Rad), following the manufacturer's protocol. qRT-PCR analysis was performed in triplicate using iQ SYBR green Supermix (BioRad) on an iCycler Real-Time Detection System (Eppendorf). The mRNA level was normalized to GAPDH or 18S as a house keeping gene (see primer sequence in Supplementary Table 5). For miRNA quantification, total RNA was reverse transcribed using the miScript II RT Kit

(Qiagen). Primers specific for mouse miR-122, miR-27b, miR148a and miR-33a (Qiagen) were used and values normalized to SNORD68 (Qiagen) (see Figure 2B). For gene expression analysis with qRT-PCR, total RNA was reversely transcribed using the high-capacity cDNA RT kit (Life Technologies). RT product (corresponding to 6.75 ng input RNA), 0.25µl Taqman gene expression assay (see Supplementary Table 6) and 2.5µl Taqman Universal PCR Master Mix No AmpErase UNG (2×) were combined in a total volume of 5µl. Cycling conditions were identical to miRNA analysis. GAPDH was used as a normalisation control.

Statin Treatment in Mice and Primary Murine Hepatocytes

Six week old, female C57Bl/6 mice were purchased from Harlan Laboratories (San Pietro al Natisone, Italy) and housed at 22°C under a 12h light/dark cycle under specific pathogen-free conditions with ad libitum access to chow and water. Mice were injected once a day with 20mg/kg atorvastatin intraperitoneally (Sigma Aldrich, Taufkirchen, Germany) for five days. Mice were sacrificed on day 5. Serum was collected by cardiac puncture. The liver was perfused with ice-cold phosphate-buffered saline and tissue specimens from the left lower lobe were either snap frozen or placed in RNAlater (Qiagen, Hilden, Germany) until further processing.

For *in vitro* experiments, primary mouse hepatocytes were isolated as previously described (2). Briefly, mice were anesthetized, the abdomen was opened and liver, vena cava, and portal vein were prepared. The liver was perfused regressively from the abdominal vena cava, via the liver veins (the vena cava proximal to the liver veins was occluded with a microclamp) to the portal vein using a peristaltic pump (Bio-Rad, Hercules, CA). The liver was first perfused using liver perfusion medium 1 supplemented with 0.1mM EGTA at a flow rate of 7 ml/min for 10min. Thereafter, liver perfusion medium 2 containing 30 µg/ml

Liberase TM (Roche, Mannheim, Germany) was used at a flow rate of 3.5 ml/min for another 10min. The liver was removed carefully and transferred into a petri-dish containing L-15 medium (Gibco, Carlsbad, CA). The capsule was incised and the resulting cell suspension was passed through a 100µm cell strainer. Hepatocytes were sedimented by low-speed centrifugation at 30 × g for 3min. Purity and viability were >90% after an isodensity Percoll centrifugation. 1.3×10^5 hepatocytes per cm^2 were seeded in William's E medium supplemented with 10% FCS and penicillin/streptomycin on collagen-coated 6-well plates. After resting cells overnight, hepatocytes were exposed to 0.1, 10, and 25 µM atorvastatin for 24h. Supernatants were harvested and cells were lysed in Buffer RLT. Both were stored at -80°C until further workup.

Plasma Proteomics in the Bruneck cohort

PlasmaDive kits (Biognosys AG) were used to profile plasma proteins in the Bruneck Study. Plasma samples were processed according to the manufacturer's instructions with one exception: peptide standards were spiked in before and not after tryptic digestion and C18 clean-up. Briefly, 10µl of plasma samples were denatured, reduced and alkylated. 20µg of proteins were spiked with 100 authentic heavy peptide standards. Seven proteins were below the limit of detection. An in-solution digestion was performed overnight. After solid phase extraction with C18 spin columns (96-well format, Harvard apparatus), the eluted peptides were dried using a SpeedVac (Thermo) and resuspended in 40µl of liquid chromatography (LC) solution. The samples were analysed on an Agilent 1290 LC system interfaced to an Agilent 6495 Triple Quadrupole MS. 10µl samples were directly injected onto a 25cm column (AdvanceBio Peptide Map 2.1 x 250mm) and separated over a 23min gradient at 300µl/min. The data were analysed using Skyline software version 3.1 (MacCross Lab) and protein concentrations were calculated using the heavy/light (H/L) ratio.

Proteomics of Liver Samples from AntagomiR-122 Treated Mice

Liver tissue was homogenized using Lysing Matrix D in radioimmunoprecipitation assay buffer (RIPA buffer) and protein concentrations were determined by the bicinchoninic acid assay (BCA). 20ug of protein from each liver sample were denatured with 6M urea/2M thiourea, reduced in 10mM DTT at 37 °C for 1h, and alkylated in 50mM iodoacetamide in the dark for 1h. Proteins were precipitated with ice cold acetone overnight and resuspended in 40 µl of 0.1M TEAB buffer, pH 8.2. Trypsin was added at a trypsin:protein ratio = 1:50 and proteins were digested overnight at 37 °C in agitation. The digestion was stopped by addition of 4 µl of 10% trifluoroacetic acid (TFA). Peptide samples were purified using C18 spin plate (Harvard Apparatus). The eluted peptides were dried using SpeedVac and resuspended in 40µl of 2% ACN + 0.05% TFA resulting in a final peptide-concentration of 0.5 µg/µl.

One microgram of digested peptides was separated using nano-flow HPLC (U3000 RSLCnano, C18 column, 75um ID x 50cm, Thermo Fisher Scientific) with the following gradient: 0-10min, 4%-10% B; 10-75min, 10%-30% B; 75-80min, 30%-40% B; 80-85min, 40%-99% B; 85-90min, 99% B; 90-120min, 4% B; where A=0.1% FA and B=80% ACN, 0.1% FA. The spectra were collected on a Q Exactive HF mass spectrometer (Thermo Fisher Scientific) with full MS scan range 350-1600 m/z (resolution 60,000) and top 15 most abundant precursor ions were selected for MS/MS in Orbitrap (resolution 15,000) with dynamic exclusion enabled. The data were searched against Uniprot mouse database (downloaded from ProteinCenter, version 2015-11-11, 24875 entries) using Proteome Discoverer 2.1 with Sequest HT. The following parameters were used: precursor mass tolerance=10ppm, fragment mass tolerance=0.02Da, trypsin as digestion enzyme and 2 missed cleavages allowed, carbamidomethylation of cysteines was used as fixed modification, oxidation of methionine as variable modification. The search results were loaded into Scaffold (version 4.3.2) and total TIC of each protein was used for quantification.

For TMT labelling, 10µg of peptide digests were concentrated using a SpeedVac and re-suspended at 1µg/µl using 10µl of 50mM TEAB. TMT labelling was carried out according to the manufacturer's instruction (TMT 10plex kit, QK226224, Thermo Fisher Scientific). After labelling, 10 samples were pooled together and dried down. The combined sample, containing a total of 100µg of peptide was then re-suspended in 100µl of 2% ACN + 0.05% TFA (1µg/µl). 1µg of mixed peptides was separated using nano-flow HPLC (U3000 RSLCnano, EASY-SPRAY C18 LC column, 75um ID x 50cm, Thermo Fisher Scientific) with the following gradient: 0-3min, 4% B; 3-10min, 4%-8%B; 10-200min, 8%-30% B; 200-210min, 30%-40% B; 210-215min, 40%-99%B; 215-220%, 99% B; 220-250min, 4% B; where A=0.1% FA and B=80% ACN, 0.1% FA.

The Synchronous Precursor Selection (SPS)-MS3 method was used on an Orbitrap Fusion Lumos Tribrid mass spectrometer (Thermo Fisher): Full MS on Orbitrap, scan range 375-1500 m/z (resolution 120,000), followed by data-dependant MS2 using CID fragmentation in ion trap using top speed mode with dynamic exclusion enabled, and synchronized precursor selection (SPS)-MS3 on the top 5 ions from the MS2 spectra in Orbitrap scan range 100-500 m/z (resolution 60,000) for the reporter ion using HCD fragmentation. The data were analysed using Proteome Discoverer 2.1. Sequest HT search was performed against UniProt mouse database (downloaded from ProteinCenter, version 2015-11-11, 24875 entries) with the following parameters: precursor mass tolerance=10ppm, fragment mass tolerance=0.6Da, trypsin as digestion enzyme and 2 missed cleavages allowed, carbamidomethylation of cysteines, TMT6plex on N-terminals and lysines, were used as fixed modification, oxidation of methionine as variable modification. The S/N of reporter ions from MS3 spectra were used for quantification with normalization and scaling option enabled.

References

1. Suárez Y, Fernández-Hernando C, Pober JS, Sessa WC. Dicer dependent microRNAs regulate gene expression and functions in human endothelial cells. Circ Res 2007;100:1164–1173.
2. Moschen AR, Gerner R, Schroll A, Fritz T, Kaser A, Tilg H. A key role for Pre-B cell colony-enhancing factor in experimental hepatitis. Hepatology 2011;54:675–686.
3. Fong MY, Zhou W, Liu L, et al. Breast-cancer-secreted miR-122 reprograms glucose metabolism in premetastatic niche to promote metastasis. Nat Cell Biol 2015;17:183–194.
4. Kojima S, Gatfield D, Esau CC, Green CB. MicroRNA-122 modulates the rhythmic expression profile of the circadian deadenylase Nocturnin in mouse liver. PLoS One 2010;5:e11264.
5. Tsai WC, Hsu SD, Hsu CS, et al. MicroRNA-122 plays a critical role in liver homeostasis and hepatocarcinogenesis. J Clin Invest 2012;122:2884–2897.
6. Iliopoulos D, Drosatos K, Hiyama Y, Goldberg IJ, Zannis VI. MicroRNA-370 controls the expression of microRNA-122 and Cpt1alpha and affects lipid metabolism. J Lipid Res 2010;51:1513–1523.
7. Liu T, Huang Y, Liu J, et al. MicroRNA-122 influences the development of sperm abnormalities from human induced pluripotent stem cells by regulating TNP2 expression. Stem Cells Dev 2013;22:1839–1850.
8. Kojima K, Takata A, Vadnais C, et al. MicroRNA122 is a key regulator of α-fetoprotein expression and influences the aggressiveness of hepatocellular carcinoma. Nat Commun 2011;2:338.
9. Davoodian N, Lotfi AS, Soleimani M, Mowla SJ. MicroRNA-122 overexpression promotes hepatic differentiation of human adipose tissue-derived stem cells. J Cell Biochem 2014;115:1582–1593.
10. Tanimizu N, Kobayashi S, Ichinohe N, Mitaka T. Downregulation of miR122 by grainyhead-like 2 restricts the hepatocytic differentiation potential of adult liver progenitor cells. Development 2014;141:4448–4456.

Supplementary Table 1 – Effect of antagomiR-122 injection on the hepatic proteome assessed using label-free proteomics. Proteins with P<0.05 are listed. Proteins that were also identified using proteomics with TMT-labelling are shown in **bold**.

Protein name	Accession Number	UniProt ID	Total TIC		Standardised mean difference	P value (unpaired t-test)
			Ctrl-miR (x10^6)	Anti-miR122 (x10^6)		
Nascent polypeptide-associated complex subunit alpha	Q60817	NACA_MOUSE	85±31	186±32	1.66	0.0009
Nascent polypeptide-associated complex subunit alpha, muscle-specific form	P70670	NACAM_MOUSE (+1)	85±31	186±32	1.66	0.0009
Dolichol-phosphate mannosyltransferase subunit 3	Q9D1Q4	DPM3_MOUSE	5±0	12±2	1.81	0.0015
Tropomyosin alpha-4 chain	Q6IRU2	TPM4_MOUSE	10±6	26±4	1.64	0.0015
Glucokinase	P52792-1	HXK4_MOUSE	15±7	103±29	1.75	0.0017
Isoform 2 of Glucokinase	P52792-2	HXK4_MOUSE	15±7	103±29	1.75	0.0017
Major vault protein	Q9EQK5	MVP_MOUSE	82±20	134±17	1.61	0.0021
ATP synthase F(0) complex subunit B1, mitochondrial	Q9CQQ7	AT5F1_MOUSE	572±103	922±145	1.60	0.0029
Importin-7	Q9EPL8	IPO7_MOUSE	15±2	25±1	1.78	0.0033
60S ribosomal protein L10A	P53026	RL10A_MOUSE	228±67	380±35	1.61	0.0040
NADH dehydrogenase [ubiquinone] iron-sulfur protein 2, mitochondrial	Q91WD5	NDUS2_MOUSE	150±23	94±22	-1.54	0.0046
Constitutive coactivator of PPAR-gamma-like protein 1	Q6A0A9	F120A_MOUSE	14±9	33±5	1.57	0.0047
Phenylalanine--tRNA ligase alpha subunit	Q8C0C7	SYFA_MOUSE	26±8	53±12	1.57	0.0047
Proteasome subunit beta type-8	P28063	PSB8_MOUSE	17±4	36±7	1.67	0.0052
Apolipoprotein B-100	E9Q414	APOB_MOUSE	14±10	35±6	1.54	0.0058
Isoleucine--tRNA ligase, cytoplasmic	Q8BU30	SYIC_MOUSE	27±6	14±5	-1.52	0.0058
Carnitine O-palmitoyltransferase 1, liver isoform	**P97742**	**CPT1A_MOUSE**	**164±42**	**254±36**	**1.50**	**0.0066**
Prosaposin	Q61207	SAP_MOUSE	808±163	1408±301	1.54	0.0074
V-type proton ATPase subunit G 1	Q9CR51	VATG1_MOUSE	39±9	59±9	1.47	0.0088
Carbonic anhydrase 2	P00920	CAH2_MOUSE	176±42	93±32	-1.48	0.0088
Guanine nucleotide-binding protein subunit beta-2-like 1	P68040	GBLP_MOUSE	524±69	672±68	1.46	0.0092
Ras GTPase-activating protein-binding protein 1	P97855	G3BP1_MOUSE	26±8	42±6	1.47	0.0095
Solute carrier family 22 member 1	O08966	S22A1_MOUSE	25±5	34±4	1.45	0.0098
Tubulin beta-5 chain	P99024	TBB5_MOUSE	55±47	142±29	1.48	0.0101
Haloacid dehalogenase-like hydrolase domain-containing protein 3	Q9CYW4	HDHD3_MOUSE	49±26	97±12	1.52	0.0104
Isoform 3 of Sec1 family domain-containing protein 1	Q8BRF7-3	SCFD1_MOUSE	8±2	14±3	1.54	0.0111
NADPH:adrenodoxin oxidoreductase, mitochondrial	Q61578	ADRO_MOUSE	35±9	13±8	-1.55	0.0111
Sec1 family domain-containing protein 1	Q8BRF7	SCFD1_MOUSE	8±2	14±3	1.54	0.0111
Isoform 2 of Leukemia inhibitory factor receptor	P42703-2	LIFR_MOUSE	94±23	350±28	1.71	0.0115
Leukemia inhibitory factor receptor	P42703-1	LIFR_MOUSE	94±23	350±28	1.71	0.0115

Supplementary Table 1 (cont'd)

Protein name	Accession Number	UniProt ID	Total TIC		Standardised mean difference	P value (unpaired t-test)
			Ctrl-miR (x10^6)	Anti-miR122 (x10^6)		
Dynein light chain 2, cytoplasmic	Q9D0M5	DYL2_MOUSE	69±58	174±37	1.46	0.0117
L-lactate dehydrogenase C chain	P00342	LDHC_MOUSE	2680±228	3250±252	1.52	0.0118
Mitochondrial pyruvate carrier 2	Q9D023	MPC2_MOUSE	326±23	157±90	-1.56	0.0118
ATP-dependent RNA helicase DDX1	Q91VR5	DDX1_MOUSE	16±12	39±3	1.56	0.0122
Prolow-density lipoprotein receptor-related protein 1	**Q91ZX7**	**LRP1_MOUSE**	**15±3**	**58±22**	**1.57**	**0.0124**
40S ribosomal protein S16	**P14131**	**RS16_MOUSE**	**258±75**	**446±104**	**1.44**	**0.0128**
Putative L-aspartate dehydrogenase	Q9DCQ2	ASPD_MOUSE	298±29	206±52	-1.47	0.0129
Isoform 2 of Polyadenylate-binding protein 2	Q8CCS6-2	PABP2_MOUSE	10±1	4±2	-1.67	0.0134
Polyadenylate-binding protein 2	Q8CCS6	PABP2_MOUSE	10±1	4±2	-1.67	0.0134
28S ribosomal protein S31, mitochondrial	Q61733	RT31_MOUSE	37±4	23±3	-1.67	0.0134
Lysozyme c-2	P08905	LYZ2_MOUSE	5±1	13±1	1.71	0.0135
Lysozyme c-1	P17897	LYZ1_MOUSE	5±1	13±1	1.71	0.0135
GDH/6PGL endoplasmic bifunctional protein	Q8CFX1	G6PE_MOUSE	83±20	123±20	1.41	0.0135
S-methyl-5'-thioadenosine phosphorylase	Q9CQ65	MTAP_MOUSE	11±4	30±8	1.65	0.0137
Profilin-1	P62962	PROF1_MOUSE	302±114	510±101	1.39	0.0161
Endoplasmin	P08113	ENPL_MOUSE	1062±226	1500±235	1.38	0.0170
40S RIBOSOMAL PROTEIN S6	P62754	RS6_MOUSE	364±33	558±115	1.50	0.0173
Peptidyl-prolyl cis-trans isomerase FKBP5	Q64378	FKBP5_MOUSE	6±1	14±5	1.44	0.0174
Lactoylglutathione lyase	Q9CPU0	LGUL_MOUSE	764±120	1140±230	1.43	0.0176
Ran-specific GTPase-activating protein	P34022	RANG_MOUSE	25±8	38±4	1.43	0.0177
Isoform HSP105-beta of Heat shock protein 105 kDa	Q61699-2	HS105_MOUSE	17±7	30±7	1.38	0.0178
Heat shock protein 105 kDa	Q61699	HS105_MOUSE	17±7	30±7	1.38	0.0178
Isoform 2 of 1-phosphatidylinositol 4,5-bisphosphate phosphodiesterase eta-1	Q4KWH5-2	PLCH1_MOUSE	87±64	194±45	1.39	0.0179
Isoform 3 of 1-phosphatidylinositol 4,5-bisphosphate phosphodiesterase eta-1	Q4KWH5-3	PLCH1_MOUSE	87±64	194±45	1.39	0.0179
Isoform 4 of 1-phosphatidylinositol 4,5-bisphosphate phosphodiesterase eta-1	Q4KWH5-4	PLCH1_MOUSE	87±64	194±45	1.39	0.0179
1-phosphatidylinositol 4,5-bisphosphate phosphodiesterase eta-1	Q4KWH5	PLCH1_MOUSE	87±64	194±45	1.39	0.0179
ADP/ATP translocase 1	P48962	ADT1_MOUSE	1700±412	2400±316	1.38	0.0181
Sodium/potassium-transporting ATPase subunit beta-1	P14094	AT1B1_MOUSE	46±29	93±17	1.41	0.0184
Regulator of microtubule dynamics protein 2	Q8BSE0	RMD2_MOUSE	14±3	39±16	1.44	0.0195
Isoform RRp2 of Ribosome-binding protein 1	Q99PL5-10	RRBP1_MOUSE	142±25	290±92	1.47	0.0204
Isoform RRp5.4 of Ribosome-binding protein 1	Q99PL5-9	RRBP1_MOUSE	142±25	290±92	1.47	0.0204
Protein LYRIC	Q80WJ7	LYRIC_MOUSE	9±3	21±8	1.40	0.0208

Supplementary Table 1 (cont'd)

Protein name	Accession Number	UniProt ID	Total TIC		Standardised mean difference	P value (unpaired t-test)
			Ctrl-miR (x10^6)	Anti-miR122 (x10^6)		
Cytoplasmic dynein 1 heavy chain 1	Q9JHU4	DYHC1_MOUSE	13±7	28±9	1.35	0.0225
La-related protein 1	Q6ZQ58-1	LARP1_MOUSE	49±7	30±10	-1.45	0.0228
Aldehyde dehydrogenase family 16 member A1	Q571I9	A16A1_MOUSE	45±25	89±25	1.33	0.0233
DnaJ homolog subfamily C member 10	Q9DC23	DJC10_MOUSE	20±5	46±9	1.65	0.0239
Mitochondrial 2-oxoglutarate/malate carrier protein	Q9CR62	M2OM_MOUSE	38±11	76±26	1.40	0.0253
60S ribosomal protein L37a	**P61514**	**RL37A_MOUSE**	**52±17**	**107±37**	**1.39**	**0.0254**
40S ribosomal protein S18	**P62270**	**RS18_MOUSE**	**420±112**	**602±96**	**1.32**	**0.0254**
Isoform RRp1.8 of Ribosome-binding protein 1	Q99PL5-11	RRBP1_MOUSE	152±24	290±92	1.43	0.0262
Isoform RRp0 of Ribosome-binding protein 1	Q99PL5-12	RRBP1_MOUSE	152±24	290±92	1.43	0.0262
Isoform RRp61 of Ribosome-binding protein 1	Q99PL5-2	RRBP1_MOUSE	184±31	308±84	1.40	0.0265
Isoform RRp47 of Ribosome-binding protein 1	Q99PL5-3	RRBP1_MOUSE	184±31	308±84	1.40	0.0265
Isoform RRp41 of Ribosome-binding protein 1	Q99PL5-4	RRBP1_MOUSE	184±31	308±84	1.40	0.0265
Isoform RRp16.8 of Ribosome-binding protein 1	Q99PL5-5	RRBP1_MOUSE	184±31	308±84	1.40	0.0265
Isoform RRp15a of Ribosome-binding protein 1	Q99PL5-6	RRBP1_MOUSE	184±31	308±84	1.40	0.0265
Isoform RRp15b of Ribosome-binding protein 1	Q99PL5-7	RRBP1_MOUSE	184±31	308±84	1.40	0.0265
Isoform RRp10 of Ribosome-binding protein 1	Q99PL5-8	RRBP1_MOUSE	184±31	308±84	1.40	0.0265
Mitochondrial coenzyme A transporter SLC25A42	Q8R0Y8	S2542_MOUSE	6±2	18±8	1.37	0.0267
Aldehyde dehydrogenase, dimeric NADP-preferring	P47739	AL3A1_MOUSE	46±16	144±67	1.37	0.0269
Cytochrome P450 2A12	**P56593**	**CP2AC_MOUSE**	**198±51**	**348±103**	**1.37**	**0.0271**
Isoform 3 of APOBEC1 complementation factor	Q5YD48-3	A1CF_MOUSE	7±1	11±3	1.36	0.0275
Eukaryotic translation initiation factor 3 subunit D	O70194	EIF3D_MOUSE	9±2	22±8	1.43	0.0276
bone marrow stromal antigen 2	Q8R2Q8	BST2_MOUSE	10±2	6±2	-1.53	0.0277
Pyridoxal kinase	Q8K183	PDXK_MOUSE	122±32	73±25	-1.31	0.0278
Tetratricopeptide repeat protein 39C	Q8VE09	TT39C_MOUSE	29±21	66±16	1.42	0.0293
Phosphate carrier protein, mitochondrial	Q8VEM8	MPCP_MOUSE	420±277	824±52	1.42	0.0298
Ras-related protein Rab-8B	P61028	RAB8B_MOUSE	22±6	10±5	-1.43	0.0301
Isoform Alpha of LIM domain and actin-binding protein 1	Q9ERG0-2	LIMA1_MOUSE	16±5	34±13	1.37	0.0305
ADP-dependent glucokinase	Q8VDL4	ADPGK_MOUSE	9±1	5±1	-1.70	0.0307
Isoform 3 of ADP-dependent glucokinase	Q8VDL4-3	ADPGK_MOUSE	9±1	5±1	-1.70	0.0307
60S ribosomal protein L13a	P19253	RL13A_MOUSE	157±115	390±158	1.30	0.0309
Clathrin light chain A	O08585	CLCA_MOUSE	18±9	34±10	1.29	0.0311
Nicotinamide phosphoribosyltransferase	Q99KQ4	NAMPT_MOUSE	32±10	46±6	1.31	0.0315

Supplementary Table 1 (cont'd)

Protein name	Accession Number	UniProt ID	Total TIC		Standardised mean difference	P value (unpaired t-test)
			Ctrl-miR (x10^6)	Anti-miR122 (x10^6)		
Isocitrate dehydrogenase [NADP], mitochondrial	P54071	IDHP_MOUSE	514±58	616±66	1.28	0.0321
Isoform 2 of Peroxisomal acyl-coenzyme A oxidase 1	Q9R0H0-2	ACOX1_MOUSE	102±69	3±3	-1.33	0.0323
14 kDa phosphohistidine phosphatase	Q9DAK9	PHP14_MOUSE	24±16	61±19	1.46	0.0329
40S ribosomal protein S28	P62858	RS28_MOUSE	290±55	374±48	1.28	0.0329
60S ribosomal protein L10-like	P86048	RL10L_MOUSE	412±147	616±76	1.32	0.0332
Isoform 2 of Protein FAM63A	Q76LS9-2	FA63A_MOUSE	6±4	21±6	1.60	0.0336
Protein FAM63A	Q76LS9-1	FA63A_MOUSE	6±4	21±6	1.60	0.0336
Isoform 2 of Sulfotransferase family cytosolic 1B member 1	Q9QWG7-2	ST1B1_MOUSE	16±9	30±1	1.32	0.0340
Sulfotransferase family cytosolic 1B member 1	Q9QWG7-1	ST1B1_MOUSE	16±9	30±1	1.32	0.0340
60S ribosomal protein L23a	**P62751**	**RL23A_MOUSE**	**340±97**	**550±150**	**1.29**	**0.0348**
Medium-chain specific acyl-CoA dehydrogenase, mitochondrial	P45952	ACADM_MOUSE	502±100	640±57	1.30	0.0350
Cytochrome P450 2J5	O54749	CP2J5_MOUSE	20±7	35±10	1.29	0.0351
Isoform 2 of Clustered mitochondria protein homolog	Q5SW19-2	CLU_MOUSE	15±3	10±3	-1.27	0.0352
40S ribosomal protein S8	P62242	RS8_MOUSE	666±71	816±107	1.29	0.0354
Protein lin-7 homolog C	O88952	LIN7C_MOUSE	17±16	80±42	1.36	0.0356
Ras-related protein Rab-11B	P46638	RB11B_MOUSE	92±26	131±24	1.26	0.0360
serine/threonine-protein phosphatase PP1-alpha catalytic subunit	P62137	PP1A_MOUSE	10±3	35±18	1.35	0.0365
Glutathione S-transferase theta-2	Q61133	GSTT2_MOUSE	79±27	116±9	1.35	0.0368
40S ribosomal protein S11	P62281	RS11_MOUSE	318±35	472±114	1.35	0.0368
Acyl-coenzyme A thioesterase 13	Q9CQR4	ACO13_MOUSE	67±13	100±25	1.30	0.0376
Lysosome-associated membrane glycoprotein 1	P11438	LAMP1_MOUSE	89±27	137±30	1.31	0.0378
Transitional endoplasmic reticulum ATPase	Q01853	TERA_MOUSE	498±69	614±78	1.25	0.0380
Isoform 2 of AP-2 complex subunit beta	Q9DBG3-2	AP2B1_MOUSE	24±8	42±13	1.28	0.0385
AP-2 complex subunit beta	Q9DBG3	AP2B1_MOUSE	24±8	42±13	1.28	0.0385
Aromatic-L-amino-acid decarboxylase	O88533	DDC_MOUSE	119±49	184±24	1.30	0.0387
Peroxiredoxin-6	O08709	PRDX6_MOUSE	1440±230	1760±167	1.26	0.0388
Nucleoside diphosphate kinase 3	Q9WV85	NDK3_MOUSE	13±1	27±8	1.45	0.0392
40S ribosomal protein S13	P62301	RS13_MOUSE	398±85	526±79	1.25	0.0393
Mannose-1-phosphate guanyltransferase alpha	Q922H4	GMPPA_MOUSE	8±5	15±4	1.25	0.0394
N-acyl-aromatic-L-amino acid amidohydrolase (carboxylate-forming)	Q91XE4	ACY3_MOUSE	93±41	150±29	1.26	0.0396
Granulins	**P28798**	**GRN_MOUSE**	**73±52**	**142±28**	**1.29**	**0.0397**
Aldehyde oxidase 3	G3X982	AOXC_MOUSE	370±117	558±126	1.24	0.0403

Supplementary Table 1 (cont'd)

Protein name	Accession Number	UniProt ID	Total TIC		Standardised mean difference	P value (unpaired t-test)
			Ctrl-miR (x10^6)	Anti-miR122 (x10^6)		
Isoform Short of Heterogeneous nuclear ribonucleoprotein A1	P49312-2	ROA1_MOUSE	47±16	80±25	1.26	0.0420
proteasome subunit beta type-2	Q9R1P3	PSB2_MOUSE	44±22	73±12	1.27	0.0425
Isoform 2 of RNA-binding protein 14	Q8C2Q3-2	RBM14_MOUSE	9±2	6±1	-1.40	0.0426
RNA-binding protein 14	Q8C2Q3	RBM14_MOUSE	9±2	6±1	-1.40	0.0426
Isoform 2 of Galectin-9	O08573-2	LEG9_MOUSE	149±73	286±102	1.24	0.0427
Isoform 3 of Galectin-9	O08573-3	LEG9_MOUSE	149±73	286±102	1.24	0.0427
Galectin-9	O08573	LEG9_MOUSE	149±73	286±102	1.24	0.0427
UV excision repair protein RAD23 homolog B	P54728	RD23B_MOUSE	34±6	58±19	1.33	0.0427
60S ribosomal protein L7	P14148	RL7_MOUSE	504±61	622±89	1.24	0.0434
Isoform 3 of Microtubule-associated protein 4	P27546-3	MAP4_MOUSE	10±3	20±8	1.30	0.0435
Histidine triad nucleotide-binding protein 1	**P70349**	**HINT1_MOUSE**	**768±223**	**428±227**	**-1.23**	**0.0437**
Inorganic pyrophosphatase 2, mitochondrial	Q91VM9	IPYR2_MOUSE	29±11	61±15	1.55	0.0438
Glucose-6-phosphate 1-dehydrogenase X	Q00612	G6PD1_MOUSE	33±3	8±0	-1.72	0.0443
very long-chain acyl-CoA synthetase	O35488	S27A2_MOUSE	264±59	394±101	1.25	0.0443
Isoform 2 of Heterogeneous nuclear ribonucleoprotein A3	Q8BG05-2	ROA3_MOUSE	254±67	344±49	1.23	0.0444
Arylamine N-acetyltransferase 2	P50295	ARY2_MOUSE	5±2	8±1	1.31	0.0447
Cathepsin D	P18242	CATD_MOUSE	490±108	662±120	1.22	0.0448
Golgi reassembly-stacking protein 2	Q99JX3	GORS2_MOUSE	17±5	10±3	-1.37	0.0448
Ras-related protein Rab-11A	P62492	RB11A_MOUSE	92±26	130±25	1.22	0.0456
Myosin regulatory light chain 12B	Q3THE2	ML12B_MOUSE	98±48	158±15	1.27	0.0466
Ribonuclease inhibitor	Q91VI7	RINI_MOUSE	136±51	208±45	1.21	0.0469
UDP-glucuronosyltransferase 1-6	Q64435	UD16_MOUSE	69±65	170±71	1.21	0.0469
Peptidyl-tRNA hydrolase 2, mitochondrial	Q8R2Y8	PTH2_MOUSE	6±1	65±47	1.27	0.0470
Cathepsin B	P10605	CATB_MOUSE	368±140	560±116	1.22	0.0471
ATP-binding cassette sub-family B member 9	Q9JJ59-1	ABCB9_MOUSE	61±18	104±35	1.25	0.0485
Isoform 2 of ATP-binding cassette sub-family B member 9	Q9JJ59-2	ABCB9_MOUSE	61±18	104±35	1.25	0.0485
Gamma-butyrobetaine dioxygenase	Q924Y0	BODG_MOUSE	28±11	49±16	1.22	0.0485
Isoform 3 of Thioredoxin reductase 2, mitochondrial	Q9JLT4-3	TRXR2_MOUSE	30±8	18±7	-1.30	0.0492
NADPH--cytochrome P450 reductase	P37040	NCPR_MOUSE	252±27	292±28	1.20	0.0492
60S ribosomal protein L35	Q6ZWV7	RL35_MOUSE	226±38	364±113	1.28	0.0497

Supplementary Table 2 – Effect of antagomiR-122 injection on the hepatic proteome assessed using proteomics with TMT-labelling. Proteins with P<0.05 are listed. Proteins that were also identified using label-free proteomics are shown in **bold**.

Protein name	Accession Number	UniProt ID	Total TIC		Standardised mean difference	P value (unpaired t-test)
			Ctrl-miR (x10^6)	Anti-miR122 (x10^6)		
40S ribosomal protein S24	P16632-1	RS24_MOUSE	87.9±7.5	112.1±7.9	1.65	0.0011
Heterogeneous nuclear ribonucleoprotein L	Q8R081	HNRPL_MOUSE	113.0±9.2	87.0±6.7	-1.66	0.0012
40S ribosomal protein S29	P62274	RS29_MOUSE	89.8±8.4	110.2±6.4	1.59	0.0030
ATP synthase subunit delta, mitochondrial	Q9D3D9	ATPD_MOUSE	110.7±9.6	89.3±4.9	-1.60	0.0045
tRNA (Cytosine(34)-C(5))-methyltransferase	Q1HFZ0-1	NSUN2_MOUSE	114.3±13.1	85.7±8.9	-1.56	0.0049
Eukaryotic translation initiation factor 3 subunit L	Q8QZY1	EIF3L_MOUSE	88.7±5.6	111.3±10.7	1.57	0.0055
Ras GTPase-activating-like protein IQGAP2	Q3UQ44	IQGA2_MOUSE	92.3±6.5	107.7±6.7	1.51	0.0060
Protein-glutamine gamma-glutamyltransferase 2	P21981	TGM2_MOUSE	87.9±10.7	112.1±10.2	1.50	0.0065
Superoxide dismutase [Cu-Zn]	P08228	SODC_MOUSE	103.9±3.9	96.1±2.7	-1.51	0.0071
Serum albumin	P07724	ALBU_MOUSE	115.6±14.2	84.4±13.5	-1.49	0.0074
LIM and SH3 domain protein 1	Q61792	LASP1_MOUSE	92.8±2.6	107.2±7.0	1.58	0.0076
Actin-related protein 3	Q99JY9	ARP3_MOUSE	92.3±5.7	107.7±7.7	1.49	0.0078
Dipeptidyl peptidase 1	P97821	CATC_MOUSE	86.5±5.4	113.5±13.5	1.57	0.0081
Signal recognition particle receptor subunit alpha	Q9DBG7	SRPR_MOUSE	84.6±8.1	115.4±15.7	1.53	0.0082
Serine--tRNA ligase, cytoplasmic	P26638	SYSC_MOUSE	93.5±5.3	106.5±6.5	1.47	0.0093
Lupus La protein homolog	P32067	LA_MOUSE	92.3±5.4	107.7±8.2	1.48	0.0100
Coatomer subunit beta	Q9JIF7	COPB_MOUSE	93.3±6.5	106.7±6.5	1.43	0.0117
Myosin light polypeptide 6	Q60605	MYL6_MOUSE	91.3±6.4	108.7±9.6	1.46	0.0117
ATP synthase subunit g, mitochondrial	Q9CPQ8	ATP5L_MOUSE	103.6±3.4	96.4±3.8	-1.42	0.0133
Proteasome subunit beta type-3	Q9R1P1	PSB3_MOUSE	91.8±3.2	108.1±9.2	1.51	0.0137
60S ribosomal protein L37a	**P61514**	**RL37A_MOUSE**	**93.9±4.3**	**106.0±7.0**	**1.44**	**0.0144**
Glycerol kinase	Q64516-3	GLPK_MOUSE	93.1±6.1	106.9±7.8	1.41	0.0153
Mitochondrial glutamate carrier 1	Q9D6M3	GHC1_MOUSE	95.1±5.6	104.9±4.6	1.39	0.0164
Vigilin	Q8VDJ3	VIGLN_MOUSE	96.3±1.3	103.7±4.4	1.50	0.0168
40S ribosomal protein S18	**P62270**	**RS18_MOUSE**	**92.8±4.1**	**107.2±8.8**	**1.44**	**0.0177**
obg-like ATPase 1	Q9CZ30-1	OLA1_MOUSE	96.6±4.1	103.4±1.0	1.49	0.0191
Apolipoprotein A-I	Q00623	APOA1_MOUSE	115.8±19.6	84.3±7.2	-1.45	0.0194
Translocation protein SEC63 homolog	Q8VHE0	SEC63_MOUSE	84.6±18.6	115.4±13.6	1.38	0.0195
Estradiol 17-beta-dehydrogenase 2	P51658	DHB2_MOUSE	89.6±6.3	110.4±13.2	1.42	0.0198
Isoform LMW of Kininogen-1	O08677-2	KNG1_MOUSE	111.4±14.1	88.6±9.8	-1.37	0.0203

Supplementary Table 2 – (cont'd)

Protein name	Accession Number	UniProt ID	Total TIC		Standardised mean difference	P value (unpaired t-test)
			Ctrl-miR (x10^6)	Anti-miR122 (x10^6)		
40S ribosomal protein S16	**P14131**	**RS16_MOUSE**	**91.7±7.8**	**108.3±10.1**	**1.36**	**0.0207**
Signal recognition particle 9 kDa protein	P49962	SRP09_MOUSE	93.3±7.2	106.7±7.6	1.35	0.0209
Granulins	**P28798**	**GRN_MOUSE**	**88.0±11.7**	**111.9±14.5**	**1.35**	**0.0216**
Myosin-9	Q8VDD5	MYH9_MOUSE	91.8±9.2	108.2±9.0	1.35	0.0217
Mitochondrial ornithine transporter 1	Q9WVD5	ORNT1_MOUSE	88.1±10.0	111.9±15.4	1.36	0.0230
Protein transport protein Sec23A	Q01405	SC23A_MOUSE	93.8±7.7	106.2±6.0	1.34	0.0234
Carnitine O-palmitoyltransferase 1, liver isoform	**P97742**	**CPT1A_MOUSE**	**93.2±8.7**	**106.8±6.1**	**1.35**	**0.0235**
SEC14-like protein 4	Q8R0F9	S14L4_MOUSE	95.8±3.4	104.2±5.5	1.36	0.0244
ras-related protein Rab-7a	P51150	RAB7A_MOUSE	92.5±7.7	107.5±9.5	1.32	0.0259
60S ribosomal protein L10	Q6ZWV3	RL10_MOUSE	92.5±5.9	107.4±10.1	1.35	0.0268
Band 3 anion transport protein	P04919	B3AT_MOUSE	115.8±21.5	84.2±12.9	-1.34	0.0276
Beta-ureidopropionase	Q8VC97	BUP1_MOUSE	93.1±9.2	106.9±6.2	1.33	0.0277
CDGSH iron-sulfur domain-containing protein 3, mitochondrial	B1AR13	CISD3_MOUSE	90.6±9.8	109.4±12.0	1.31	0.0280
Ras-related protein Rab-35	Q6PHN9	RAB35_MOUSE	89.4±7.7	110.6±14.9	1.34	0.0297
60S ribosomal protein L11	Q9CXW4	RL11_MOUSE	95.2±3.7	104.8±6.8	1.33	0.0307
Monocarboxylate transporter 1	P53986	MOT1_MOUSE	84.1±8.8	116.0±23.1	1.36	0.0333
40S ribosomal protein S20	P60867	RS20_MOUSE	95.4±6.2	104.6±5.1	1.27	0.0344
Heme-binding protein 1	Q9R257	HEBP1_MOUSE	106.7±3.7	93.3±9.8	-1.35	0.0345
60S ribosomal protein L36a	P83882	RL36A_MOUSE	89.4±12.0	110.6±14.2	1.27	0.0346
Isoform 3 of Myosin-14	Q6URW6-3	MYH14_MOUSE	117.2±24.9	82.8±15.3	-1.29	0.0356
60S ribosomal protein L26	P61255	RL26_MOUSE	95.1±5.3	104.9±6.7	1.27	0.0357
26S proteasome non-ATPase regulatory subunit 3	P14685	PSMD3_MOUSE	94.8±7.3	105.2±5.3	1.28	0.0358
NADH dehydrogenase [ubiquinone] 1 alpha subcomplex subunit 2	Q9CQ75	NDUA2_MOUSE	106.0±8.6	94.0±6.0	-1.28	0.0359
Eukaryotic peptide chain release factor subunit 1	Q8BWY3	ERF1_MOUSE	110.5±13.2	89.5±13.3	-1.26	0.0365
Polypyrimidine tract-binding protein 1	P17225	PTBP1_MOUSE	93.0±9.3	107.0±8.3	1.26	0.0369
Malate dehydrogenase, cytoplasmic	P14152	MDHC_MOUSE	103.9±4.6	96.1±5.3	-1.26	0.0372
Tubulin alpha-1C chain	P68373	TBA1C_MOUSE	96.6±1.9	103.4±5.1	1.33	0.0372
peptidyl-prolyl cis-trans isomerase D	Q9CR16	PPID_MOUSE	95.1±6.5	104.9±6.0	1.25	0.0385
Clathrin heavy chain 1	Q68FD5	CLH1_MOUSE	97.7±3.1	102.3±2.9	1.25	0.0394
Thymosin beta-4	P20065	TYB4_MOUSE	83.0±6.4	117.0±25.7	1.35	0.0394
Cytosol aminopeptidase	Q9CPY7-1	AMPL_MOUSE	102.7±2.1	97.3±4.1	-1.29	0.0405
NADH dehydrogenase [ubiquinone] iron-sulfur protein 3, mitochondrial	Q9DCT2	NDUS3_MOUSE	106.9±5.0	93.1±10.6	-1.30	0.0406

Supplementary Table 2 – (cont'd)

Protein name	Accession Number	UniProt ID	Total TIC		Standardised mean difference	P value (unpaired t-test)
			Ctrl-miR (x10^6)	Anti-miR122 (x10^6)		
DNA damage-binding protein 1	Q3U1J4	DDB1_MOUSE	95.6±5.0	104.4±6.3	1.24	0.0411
Prolow-density lipoprotein receptor-related protein 1	**Q91ZX7**	**LRP1_MOUSE**	**95.2±6.6**	**104.8±5.9**	**1.24**	**0.0411**
Succinate dehydrogenase [ubiquinone] flavoprotein subunit, mitochondrial	Q8K2B3	SDHA_MOUSE	102.9±3.8	97.1±3.9	-1.24	0.0413
Fatty acid-binding protein 9	O08716	FABP9_MOUSE	84.9±16.3	115.1±22.0	1.24	0.0419
Integrin alpha-1	Q3V3R4	ITA1_MOUSE	91.2±11.4	108.8±11.6	1.23	0.0421
60S acidic ribosomal protein P1	P47955	RLA1_MOUSE	94.8±7.1	105.2±6.4	1.23	0.0426
5-hydroxyisourate hydrolase	Q9CRB3	HIUH_MOUSE	104.4±5.6	95.6±5.9	-1.23	0.0431
60S ribosomal protein L18	P35980	RL18_MOUSE	95.6±3.8	104.4±6.9	1.27	0.0435
Spliceosome RNA helicase DDX39B	Q9Z1N5	DX39B_MOUSE	94.1±6.8	105.9±8.5	1.23	0.0437
Plasminogen	P20918	PLMN_MOUSE	110.0±10.4	90.0±15.1	-1.24	0.0444
Fatty aldehyde dehydrogenase	P47740	AL3A2_MOUSE	94.5±6.1	105.5±8.2	1.23	0.0450
Succinate dehydrogenase [ubiquinone] iron-sulfur subunit, mitochondrial	Q9CQA3	SDHB_MOUSE	103.3±1.3	96.7±5.2	-1.32	0.0450
60S ribosomal protein L30	P62889	RL30_MOUSE	94.6±6.3	105.4±8.0	1.22	0.0454
Coatomer subunit alpha	Q8CIE6	COPA_MOUSE	94.6±3.0	105.5±8.7	1.30	0.0461
14-3-3 protein beta/alpha	Q9CQV8-1	1433B_MOUSE	96.8±2.5	103.2±5.1	1.26	0.0462
Histidine triad nucleotide-binding protein 1	**P70349**	**HINT1_MOUSE**	**105.7±7.9**	**94.4±7.4**	**-1.21**	**0.0475**
Alpha-1-antitrypsin 1-2	P22599	A1AT2_MOUSE	111.6±18.7	88.4±9.4	-1.25	0.0478
60S ribosomal protein L23a	**P62751**	**RL23A_MOUSE**	**92.3±7.5**	**107.7±12.2**	**1.23**	**0.0481**
Prostaglandin E synthase 3	Q9R0Q7	TEBP_MOUSE	95.4±2.7	104.6±7.4	1.28	0.0489
Cytochrome P450 2A12	**P56593**	**CP2AC_MOUSE**	**93.7±5.6**	**106.3±10.2**	**1.24**	**0.0490**
60S ribosomal protein L22	P67984	RL22_MOUSE	78.8±30.1	121.2±27.9	1.20	0.0495

Supplementary Table 3 – Predicted direct miR-122 targets and corresponding results from unlabelled and TMT-labelled proteomics.

Gene mouse (HUMAN)	Uniprot Name	Predicted mouse (x/12)	Predicted human (x/12)	Previously validated	Unlabelled proteomics	TMT-labelled proteomics
Pkm	KPYM_MOUSE	9	7	Luc Hs (3)	-	-
Aldh3a2	AL3A2_MOUSE	**6**	**5**	-	-	↑
Ccrn4l	NOCT_MOUSE	7	4	Luc Mm (4)	n.i.	n.i.
Fads1	FADS1_MOUSE	3	6	-	-	n.i.
Igf2	IGF2_MOUSE	6	3	Other Mm (5)	n.i.	n.i.
Myh9	MYH9_MOUSE	4	5	-	-	↑
Cpt1a	CPT1A_MOUSE	3	5	Other Mm (6)	↑	↑
Lgals3bp	LG3BP_MOUSE	5	3	Other Hs (7)	-	n.i.
Rab27a	RB27A_MOUSE	3	5	-	n.i.	n.i.
Tuba1c	TBA1C_MOUSE	1	7	-	-	↑
Eif3i	EIF3I_MOUSE	0	7	-	-	-
Lrp1	LRP1_MOUSE	3	4	-	↑	↑
Slc16a1	MOT1_MOUSE	5	1	-	-	↑
Slc25a15	ORNT1_MOUSE	2	4	-	-	↑
Auh	AUHM_MOUSE	4	1	-	-	-
Ldha	LDHA_MOUSE	4	1	-	-	-
Rpl23a	RL23A_MOUSE	1	4	-	↑	↑
Acsl1	ACSL1_MOUSE	2	2	-	n.i.	-
Apob	APOB_MOUSE	3	1	Other Hs (7)	↑	-
Vapa	VAPA_MOUSE	2	2	-	-	-
Iqgap2	IQGA2_MOUSE	1	2	-	-	↑
Afp	FETA_MOUSE	1	1	Other Hs (8), Other Mm (5)	n.i.	n.i.
Alb	ALBU_MOUSE	0	2	Other Hs (9), Other Mm (10)	-	↓
Apoa1	APOA1_MOUSE	1	1	-	-	↓
Asgr1	ASGR1_MOUSE	1	1	-	-	-
Grn	GRN_MOUSE	1	1	-	↑	↑
Hint1	HINT1_MOUSE	1	1	-	↓	↓
Rpl37a	RL37A_MOUSE	1	1	-	↑	↑
Cyp2a12 (CYP2A13)	CP2AC_MOUSE	0	1	-	↑	↑
Rps16	RS16_MOUSE	1	0	-	↑	↑
Rps18	RS18_MOUSE	0	0	-	↑	↑

Abbreviations: Other = Other miR-122 experiments in which the respective genes were regulated, not direct evidence for the gene being a target of miR-122; Luc = validation using luciferase assay; Hs = validation in human system or sequence; Mm = validation in mouse system or sequence; n.i. = not identified.

Supplementary Table 4 – MiRNAs in human HDL and VLDL.

	miRNA expression, C_t	
	VLDL particle	HDL particle
miR-24	28.8	32.0
miR-92a	31.8	35.8
miR-122	*Not detectable*	*Not detectable*
miR-126	30.0	29.1
miR-146a	30.9	36.1
miR-191	30.0	33.9
miR-223	23.5	24.8

MiRNAs were measured using RNA extracted from human HDL and VLDL samples. C_t, Cycle threshold.

Supplementary Table 5 – Primer sequences used to quantify expression of genes implicated in cholesterol and lipid metabolism at the mRNA level in antagomiR-122 treated mice, related to Fig. 2.

Gene	Forward (5'➔3')	Reverse (3'➔5')
18S	TTCCGATAACGAACGAGACTCT	TGGCTGAACGCCACTTGTC
Acc1	ATCCAGGCCATGTTGAGACG	AGATGTGCTGGGTCATGTGG
Acly	ATGCGAGTGCAGATCC	AAGGTAGTGCCCAATG
Aldo	TGAATAGGCTGCGTTCTCTTG	GCAGTGCTTTCCTTTCCTAACTC
Ampk	TGACCGGACATAAAGTGGCTGTGA	TGATGATGTGAGGGTGCCTGAACA
Cpt1	TTGATCAAGAAGTGCCGGACGAGT	GTCCATCATGGCCAGCACAAAGTT
Fasn	CTTCGCCAACTCTACCATGG	TTCCACACCCATGAGCGAGT
Gapdh	ACACATTGGGGGTAGGAACA	AACTTTGGCATTGTGGAAGG
Hmgcr	CTTGTGGAATGCCTTGTGATTG	AGCCGAAGCAGCACATGAT
Ldlr	GGTACTGGCAACCACCATTGGG	GCCAATCGACTCACGGGTTCAG
Mttp	AGGCAATTCGAGACAAAG	ACGTCAAAGCATATCGTTC
Scd1	CTGGAGATCTCTGGAGCATGTGGG	TACCCTTTGCTGGCAGCCGA
Srebp1	GCAGCCACCATCTAGCCTG	CAGCAGTGAGTCTCTGCCTTGAT
Srebp2	GCGTTCTGGAGACCATGGA	ACAAAGTTGCTCTGAAAACAAATCA

Supplementary Table 6 – Taqman assays used in Supplementary Fig. 3.

Gene	Taqman ID
Acsl1	Mm00484217_m1
Afm	Mm00446866_m1
Afp	Mm00431715_m1
Ahsg	Mm01145470_m1
Alb	Mm00802090_m1
Aldh3a2	Mm00839320_m1
Apoa1	Mm00437569_m1
Apob	Mm01545150_m1
Apoc2	Mm00437571_m1
Apoc3	Mm00445670_m1
Apoe	Mm01307193_g1
Asgr1	Mm01245581_m1
Auh	Mm00479363_m1
Azgp1	Mm00516331_m1
C3	Mm01232785_m1
Ccrn4l	Mm00802276_m1
Cebpa	Mm00514283_s1
Cfh	Mm01299248_m1
Cfi	Mm00432477_m1
Cpt1a	Mm01231183_m1
Crp	Mm00432680_g1
Ctsd	Mm00515586_m1
Cyp2a12	Mm00504878_m1
Eif3i	Mm00517000_m1
Fads1	Mm00507605_m1
Gapdh	Mm03302249_g1
Gpt	Mm00805379_g1
Grn	Mm00433848_m1
Hint1	Mm00801722_m1
Hp	Mm00516884_m1
Igf1	Mm00439560_m1
Igf2	Mm00439564_m1
Iqgap2	Mm01282618_m1
Ldha	Mm01612132_g1
Lgals3bp	Mm00478303_m1
Lox	Mm00495386_m1
Lrg1	Mm01278767_m1
Lrp1	Mm00464608_m1
Myh9	Mm01197036_m1
Pcsk9	Mm01263610_m1
Pkm	Mm00834102_gH
Rab27a	Mm00469997_m1
Rpl23a	Mm03020030_g1
Rpl37a	Mm01546394_s1
Rps16	Mm01617540_g1
Rps18	Mm02601777_g1
Slc16a1	Mm01306379_m1
Slc25a15	Mm01222280_m1
Sort1	Mm00490905_m1
Trib1	Mm00454875_m1
Tuba1c	Mm02528102_g1
Vapa	Mm00497141_m1
Vim	Mm01333430_m1
Vtn	Mm00495976_m1

Supplementary Figure 1 – Correlation of miR-122 over time and in serum vs. plasma in the Bruneck Study.

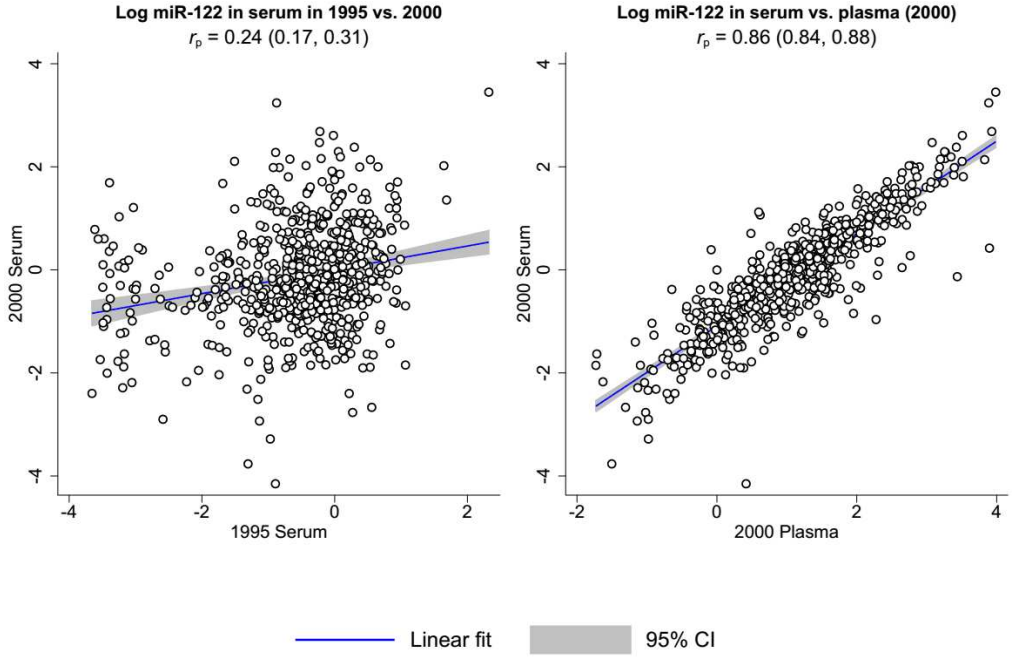

MiRNA values were log-transformed for analysis.

Supplementary Figure 2 – Correlation of serum miR-122 with circulating levels of proteins in the Bruneck Study.

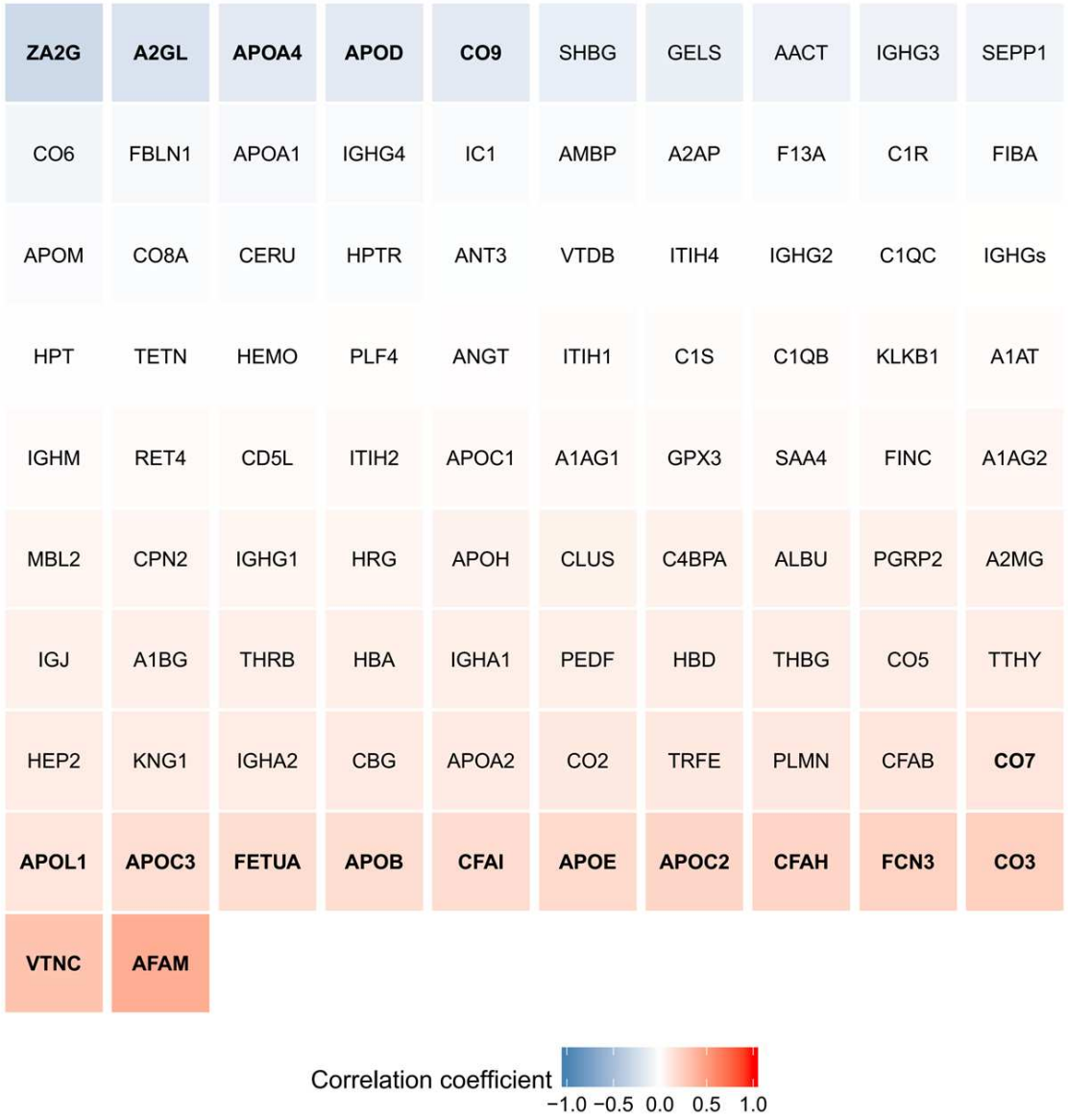

Spearman correlation coefficients were adjusted for age and sex. Proteins in bold were significant after Bonferroni-correction for multiple testing. Abbreviations: A1AG1, alpha-1-acid glycoprotein 1; A1AG2, alpha-1-acid glycoprotein 2; A1AT, alpha-1-antitrypsin; A1BG, alpha-1B-glycoprotein; A2AP, alpha-2-antiplasmin; A2GL, leucine-rich alpha-2-glycoprotein; A2MG, alpha-2-macroglobulin; AACT, alpha-1-antichymotrypsin; AFAM, afamin; ALBU, albumin; AMBP, alpha-1-microglobulin; ANGT, angiotensinogen; ANT3, antithrombin-III; APOA1, apolipoprotein A-I; APOA2, apolipoprotein A-II; APOA4, apolipoprotein A-IV; APOB, apolipoprotein B-100; APOC1, apolipoprotein C-I; APOC2, apolipoprotein C-II; APOC3, apolipoprotein C-III; APOD, apolipoprotein D; APOE, apolipoprotein E; APOH, apolipoprotein H; APOL1, apolipoprotein L1; APOM, apolipoprotein M; C1QB, complement C1q subcomponent subunit B; C1QC, complement

C1q subcomponent subunit C; C1R, complement C1r subcomponent; C1S, complement C1s subcomponent; C4BPA, C4b-binding protein alpha chain; CBG, corticosteroid-binding globulin; CD5L, CD5 antigen-like; CERU, ceruloplasmin; CFAB, complement factor B; CFAH, complement factor H; CFAI, complement factor I; CLUS, clusterin; CO2, complement C2; CO3, complement C3; CO5, complement C5; CO6, complement C6; CO7, complement C7; CO8A, complement C8 alpha chain; CO9, complement C9; CPN2, carboxypeptidase N subunit 2; F13A, coagulation factor XIII A chain; FBLN1, fibulin-1; FCN3, ficolin-3; FETUA, fetuin A; FIBA, fibrinogen alpha chain; FINC, fibronectin; GELS, gelsolin; GPX3, glutathione peroxidase 3; HBA, hemoglobin subunit alpha; HBD, hemoglobin subunit delta; HEMO, hemopexin; HEP2, heparin cofactor 2; HPT, haptoglobin; HPTR, haptoglobin-related protein; HRG, histidine-rich glycoprotein; IC1, plasma protease C1 inhibitor; IGHA1, immunoglobulin alpha 1; IGHA2, immunoglobulin alpha 2; IGHGs, immunoglobulin gamma; IGHG1, immunoglobulin gamma 1; IGHG2, immunoglobulin gamma 2; IGHG3, immunoglobulin gamma 3; IGHG4, immunoglobulin gamma 4; IGHM, immunoglobulin mu; IGJ, immunoglobulin J; ITIH1, inter-alpha-trypsin inhibitor heavy chain 1; ITIH2, inter-alpha-trypsin inhibitor heavy chain 2; ITIH4, inter-alpha-trypsin inhibitor heavy chain 4; KLKB1, kallikrein; KNG1, kininogen-1; MBL2, mannose-binding protein C; PEDF, pigment epithelium-derived factor; PGRP2, N-acetylmuramoyl-L-alanine amidase; PLF4, platelet factor 4; PLMN, plasminogen; RET4, retinol-binding protein 4; SAA4, serum amyloid A-4 protein; SEPP1, selenoprotein P; SHBG, sex hormone-binding globulin; TETN, tetranectin; THBG, thyroxine-binding globulin; THRB, prothrombin; TRFE, serotransferrin; TTHY, transthyretin; VTDB, vitamin D-binding protein; VTNC, vitronectin; ZA2G, zinc-alpha-2-glycoprotein.

Supplementary Figure 3 – (A) Volcano plots of all the qPCR data from antagomir-122 treated versus control liver samples, with the genes with P <0.05 highlighted in red. Details on the Taqman assay used is provided in Supplementary Table 6. (B) Detailed results for genes differentially expressed in the antagomiR-122 group vs. the control group, i.e. Alpha-fetoprotein, (Afp), IQ motif containing GTPase activating protein 2 (Iqgap2), and Ras-related protein (Rab27).

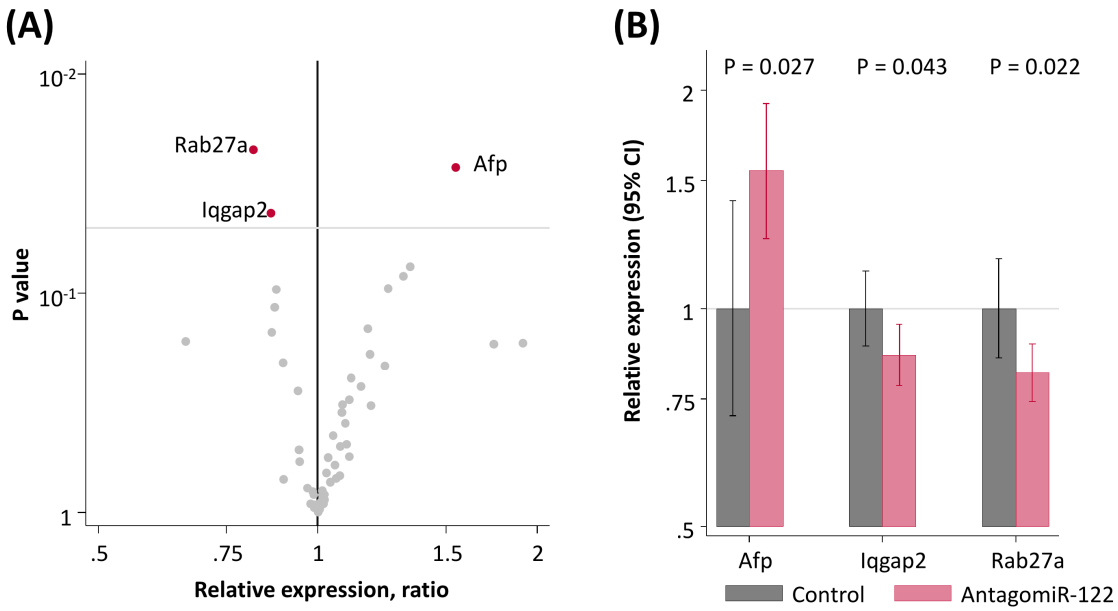

Supplementary Figure 4 – Association of miR-122 with metabolic syndrome and type-2 diabetes across clinically relevant subgroups in the Bruneck Study.

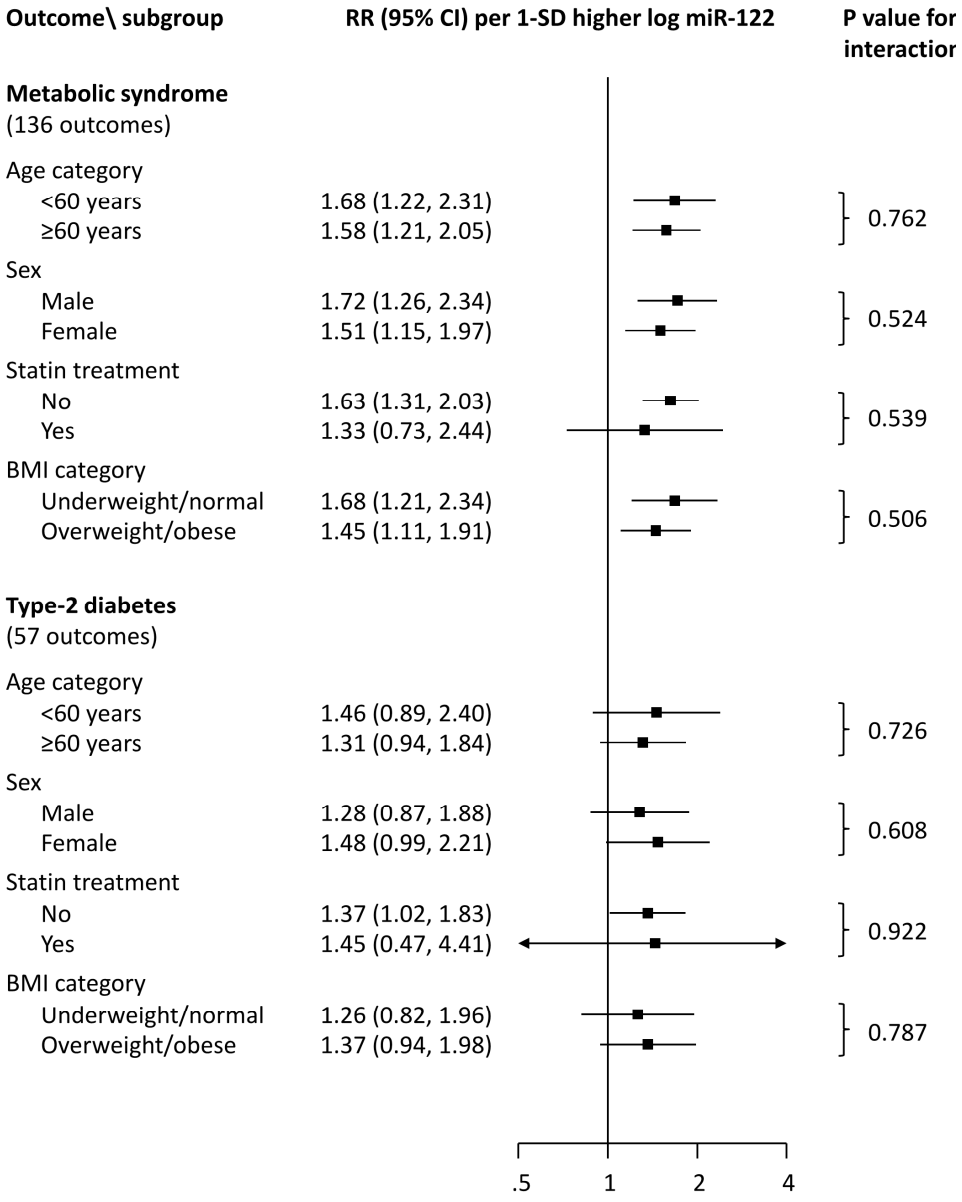

Risk ratios were adjusted for age, sex, socio-economic status, smoking, physical activity, and alcohol consumption.

Supplementary Figure 5 – Association of miR-122 with new-onset cardiovascular disease overall and across clinically relevant subgroups in the Bruneck Study.

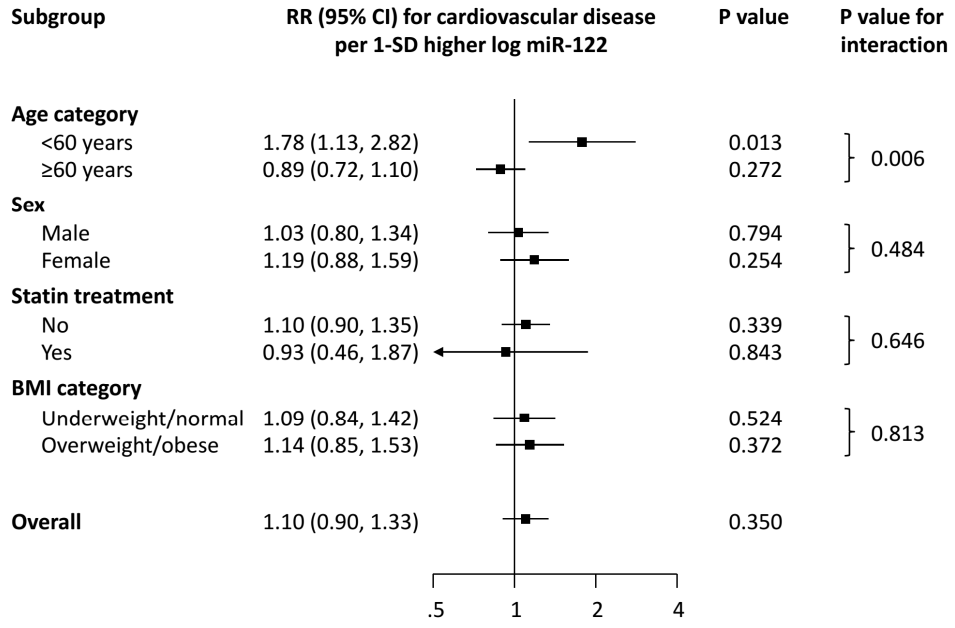

There were 108 new-onset events of cardiovascular disease. Risk ratios were adjusted for age, sex, socio-economic status, smoking, physical activity, and alcohol consumption.